Lattice QCD: from observables to physics

Paolo Giuseppe Alba

Frankfurt Institute for Advanced Studies

2nd Meeting for Heavy-Ion physics at LHC
Torino, 9th-10th October 2017

Outline

- Lattice QCD at finite density: comparison with exp.
- Criticality and Critical End Point
- Missing resonances from QCD thermodynamics
- Attractive and repulsive hadronic interactions
- Consistency with ALICE particle yields

A sea of QGP

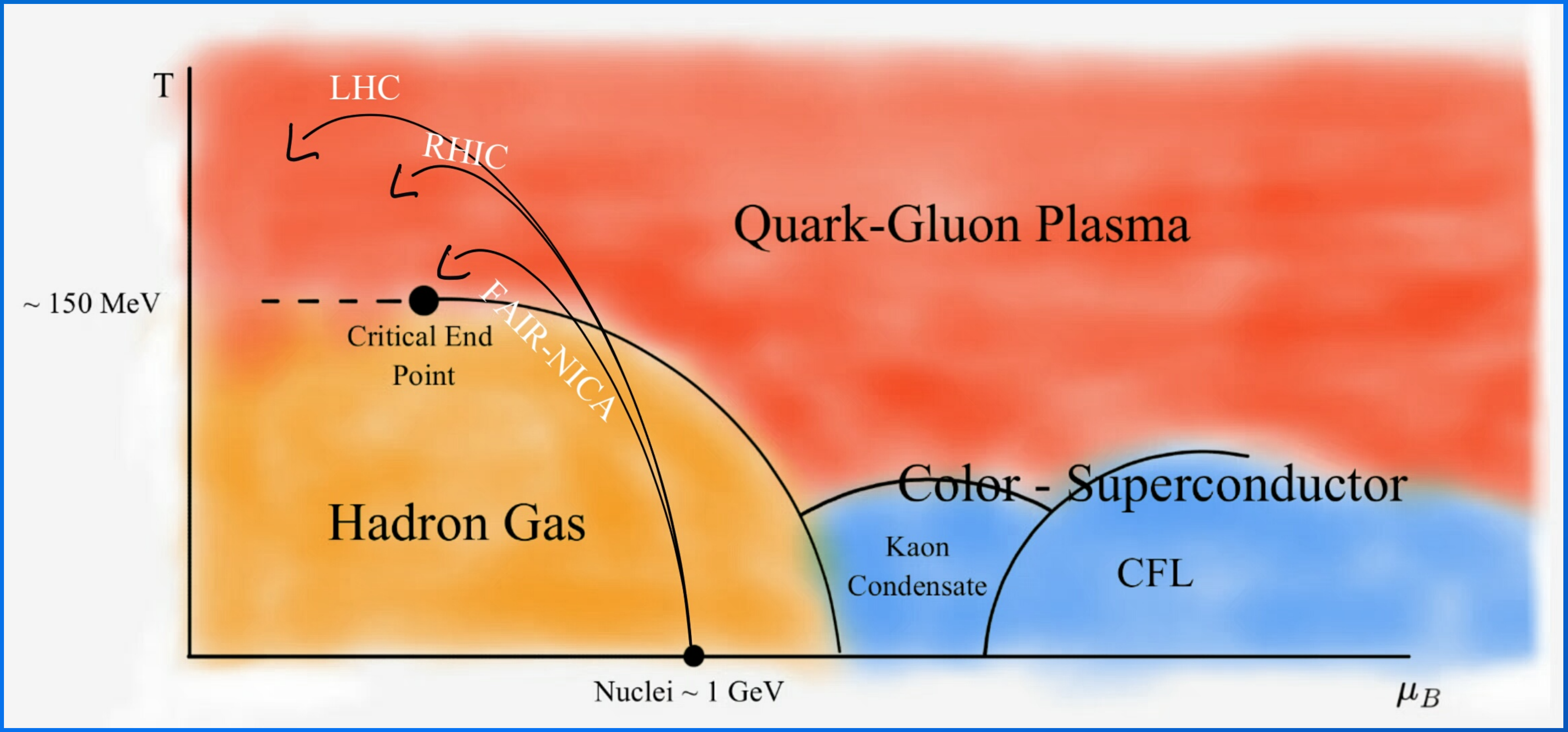

“E naufragar m’è dolce in questo Quark-Gluon Plasma ”

(and sweetly I sink in this…)

freely adapted from *L’Infinito* (the Infinity), by the italian poet *Giacomo Leopardi.*

A sea of QGP

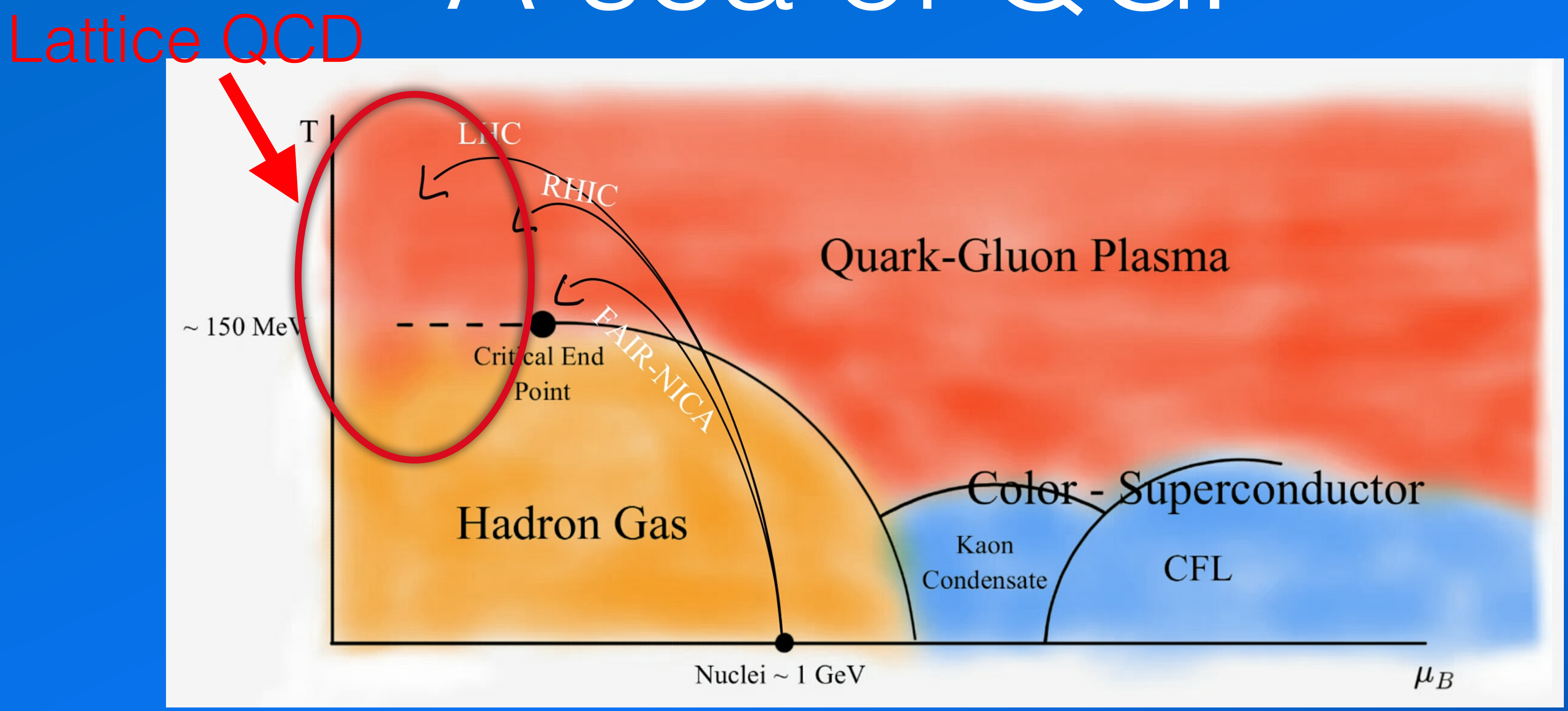

“E naufragar m’è dolce in questo Quark-Gluon Plasma ”

(and sweetly I sink in this…)

freely adapted from *L’Infinito* (the Infinity), by the Italian poet *Giacomo Leopardi.*

EoS at finite density

- Initial conditions from colliding nuclei
- Consistency between Taylor expansion and imaginary muB

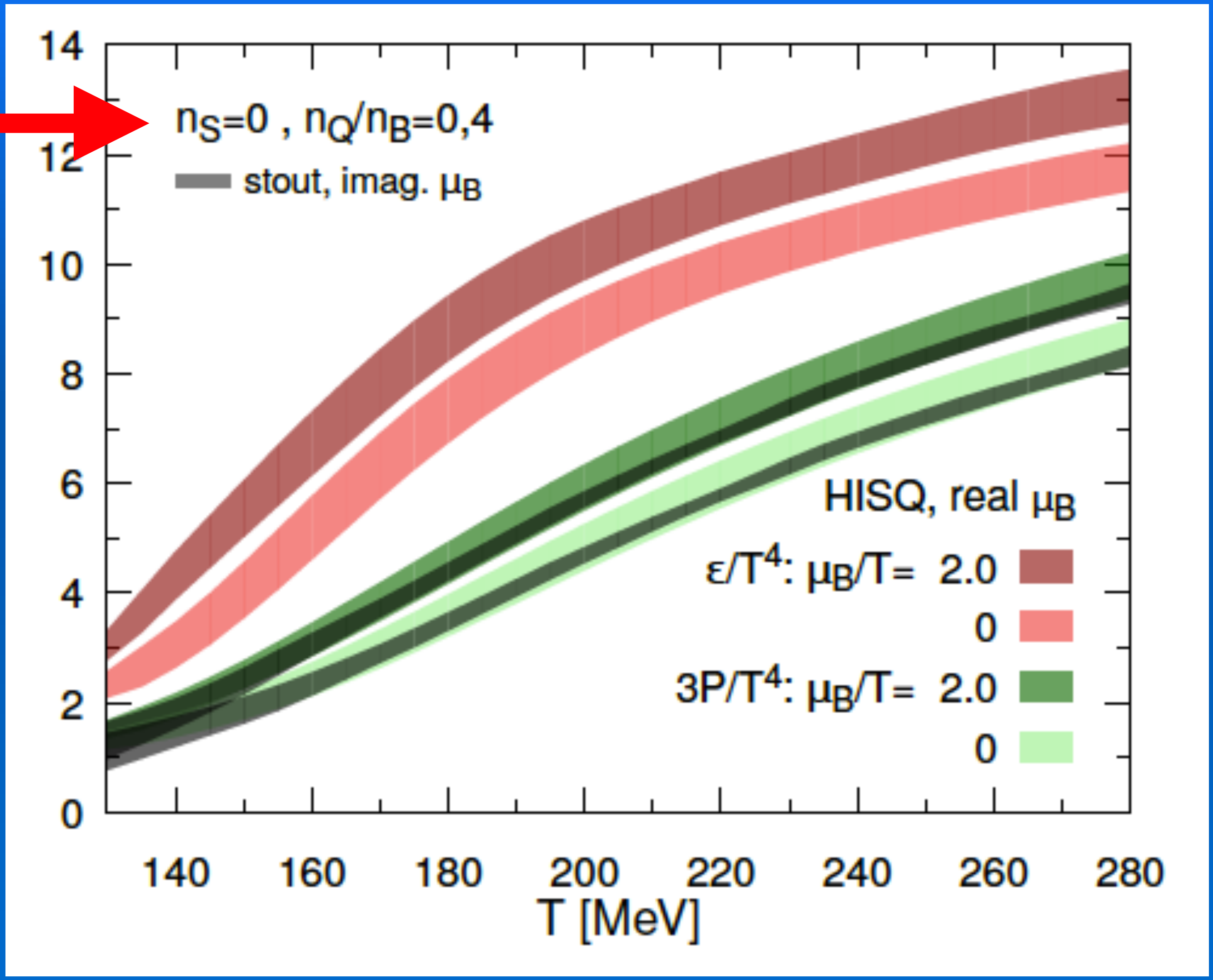

Bazavov et al., Phys.Rev. D95 (2017) no.5, 054504

EoS at finite density

For key observables, lattice can be directly compared to experiment!!!

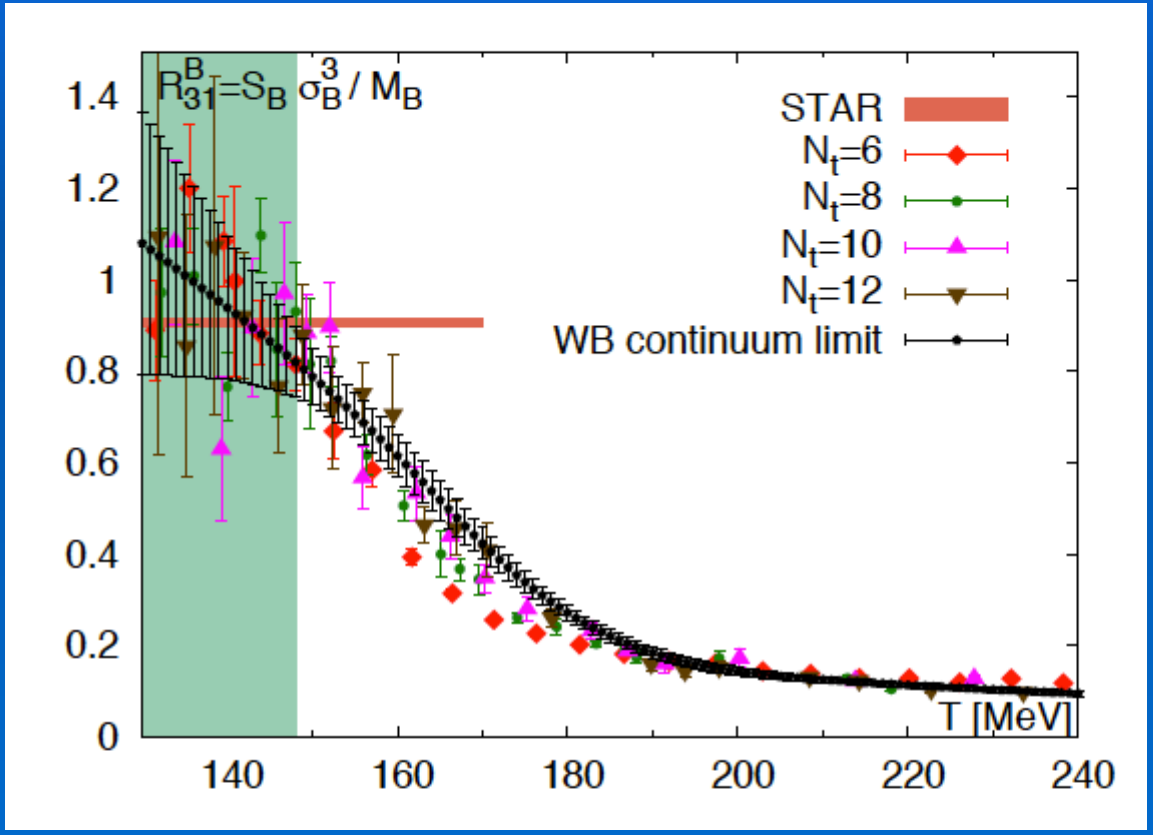

Borsanyi et al., Phys.Rev.Lett. 113 (2014) 052301

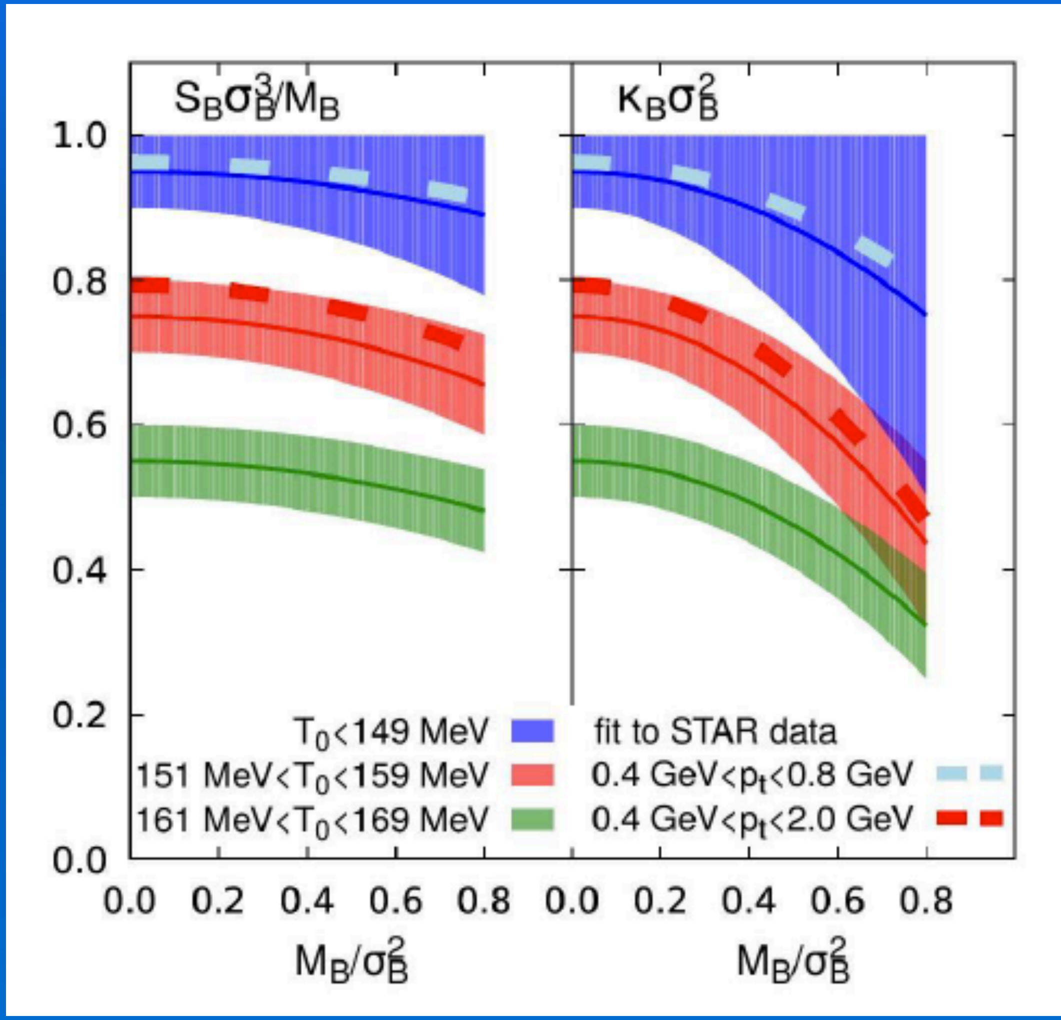

Bazavov et al., Phys.Rev. D95 (2017) no.5, 054504

EoS at finite density

Freeze-out:
constant physics

Phase transition:
inflection point

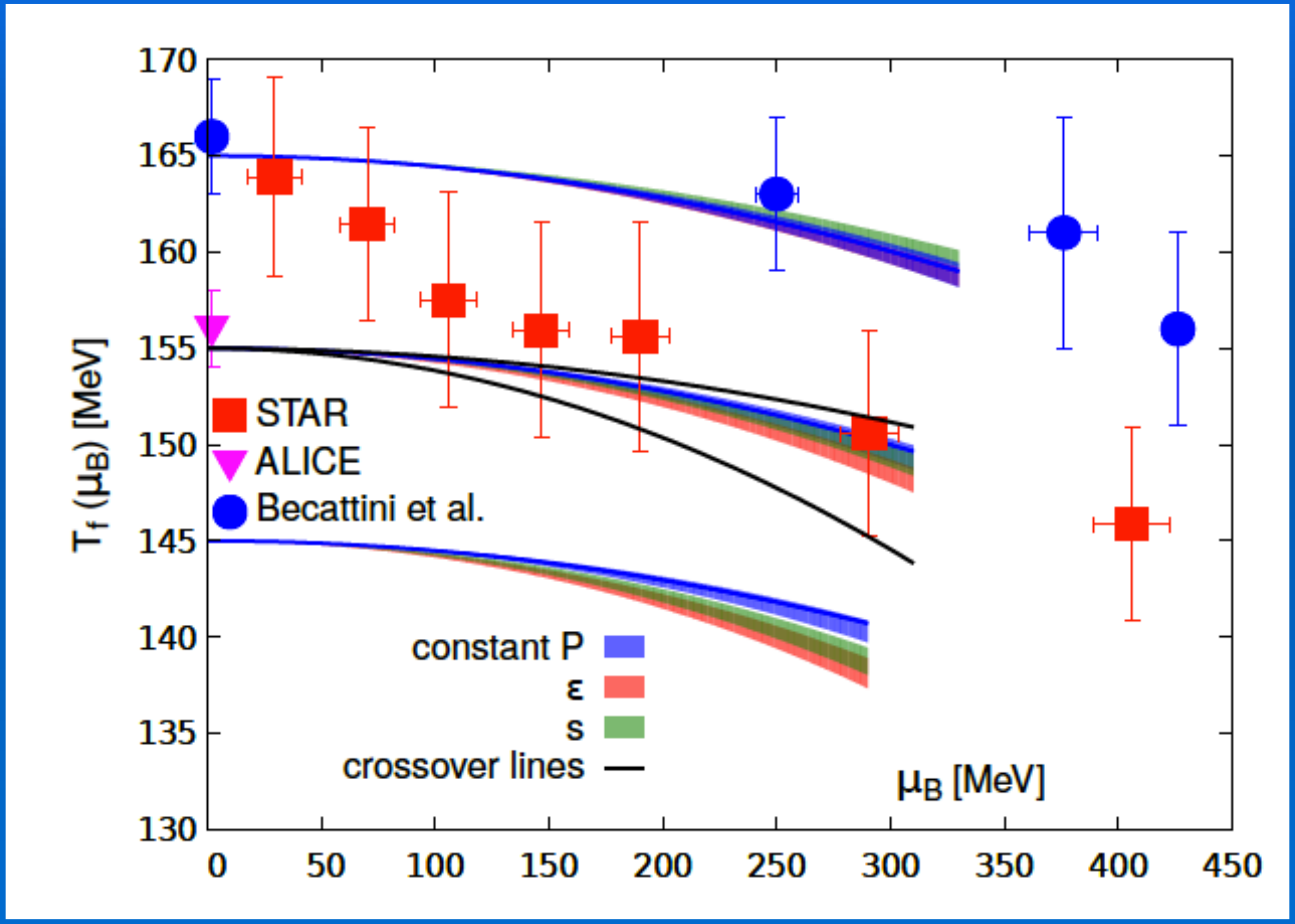

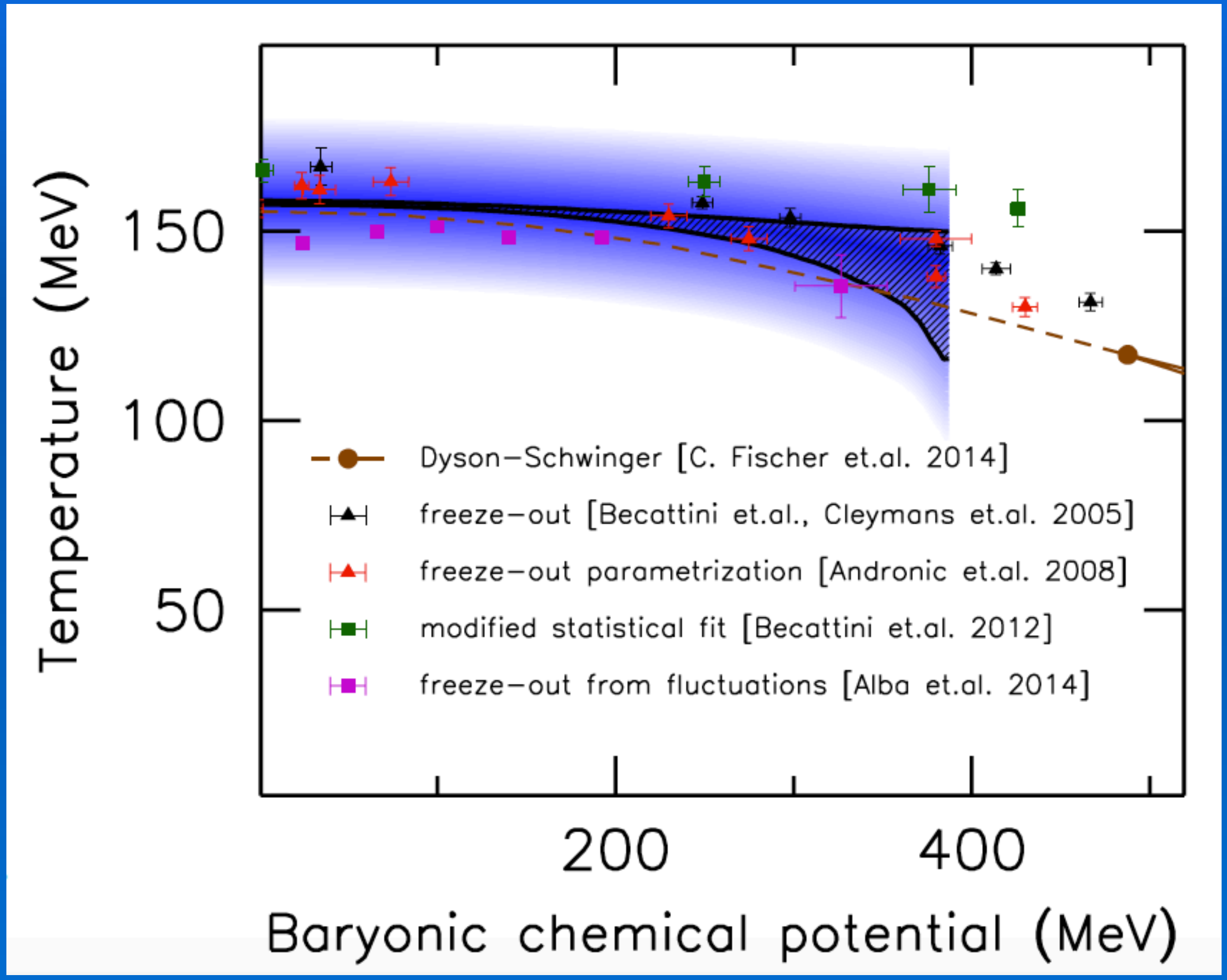

Bazavov et al., Phys.Rev. D95 (2017) no.5, 054504

Bellwied et al., Phys.Lett. B751 (2015) 559-564

Criticality and CEP

From lattice one can estimate the location of the CEP

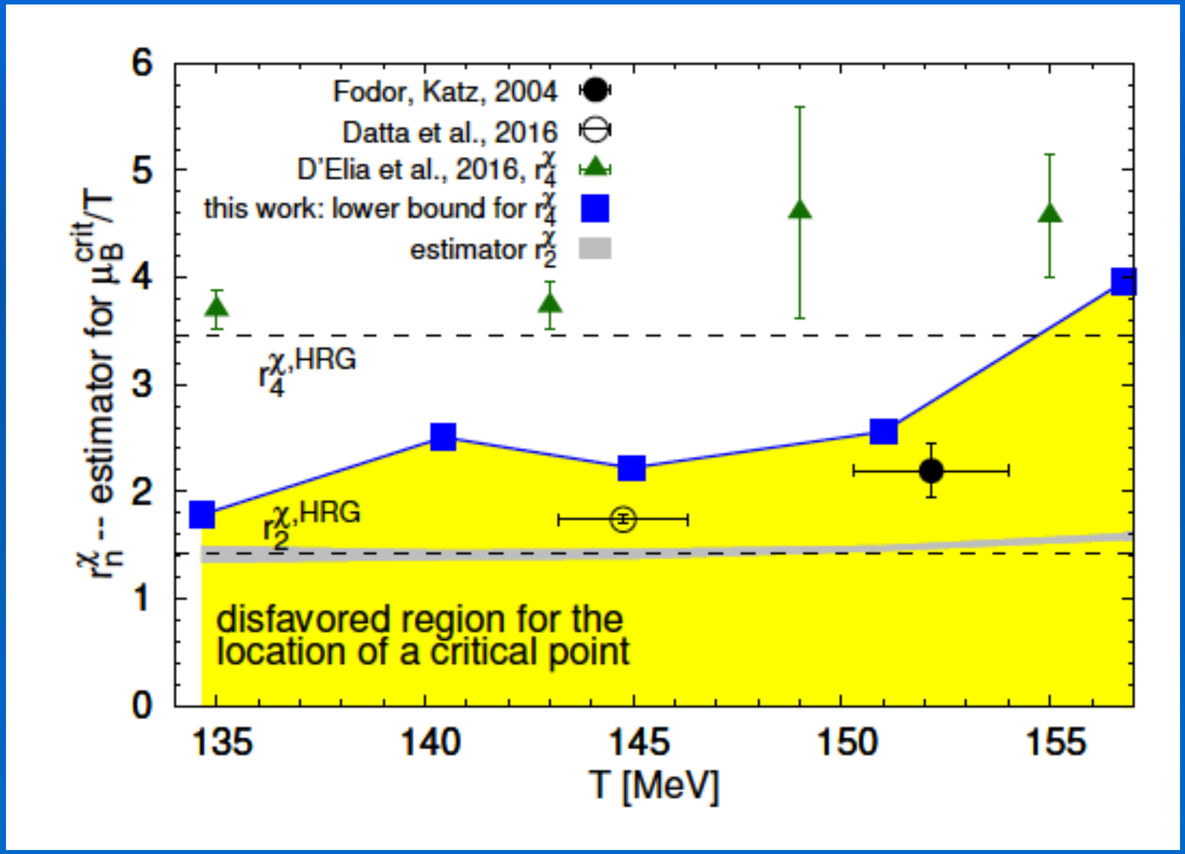

Bazavov et al., Phys.Rev. D95 (2017) no.5, 054504

Criticality and CEP

Fitting observables from lattice at vanishing muB, there is consistency in the location of the CEP

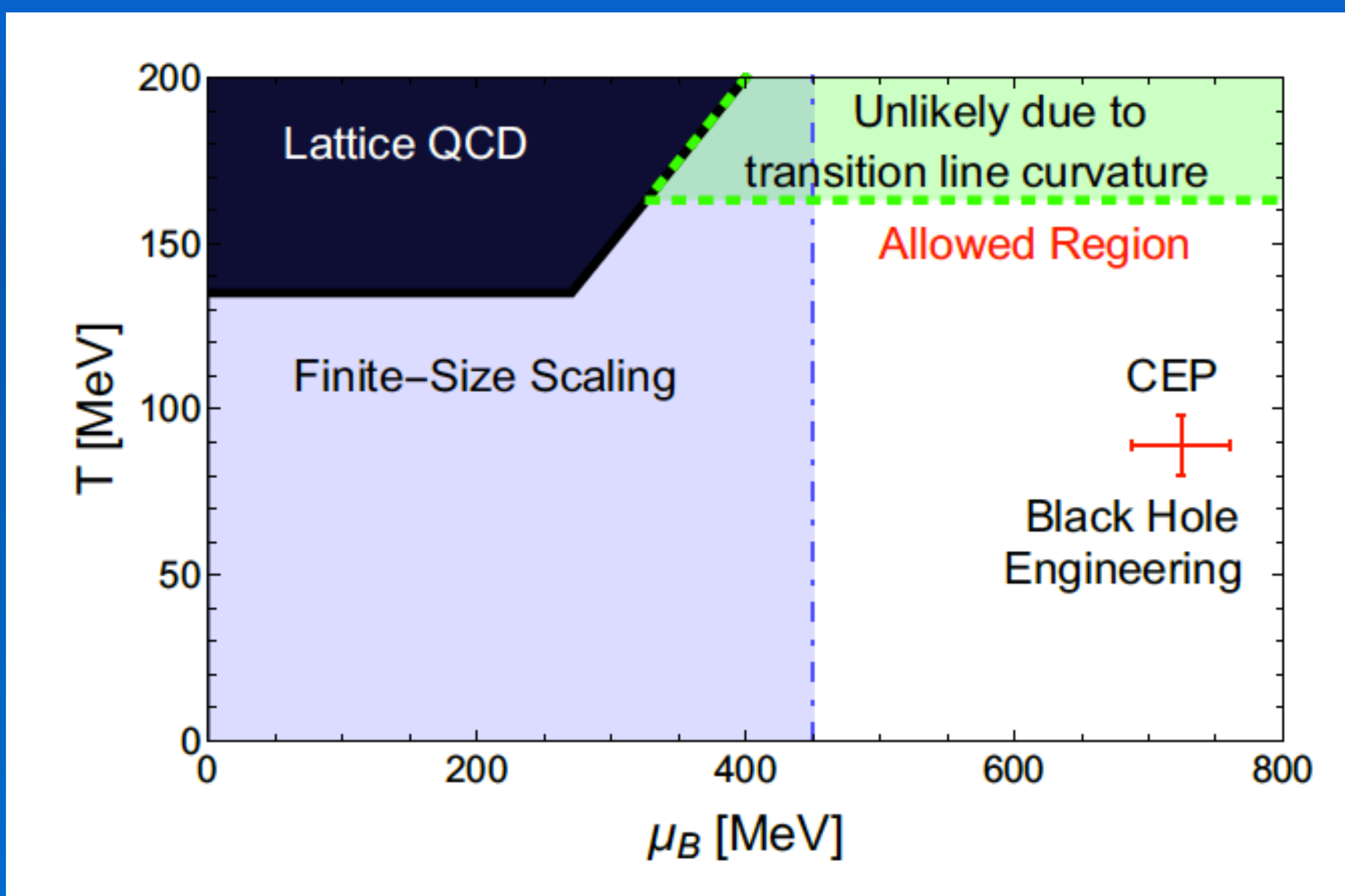

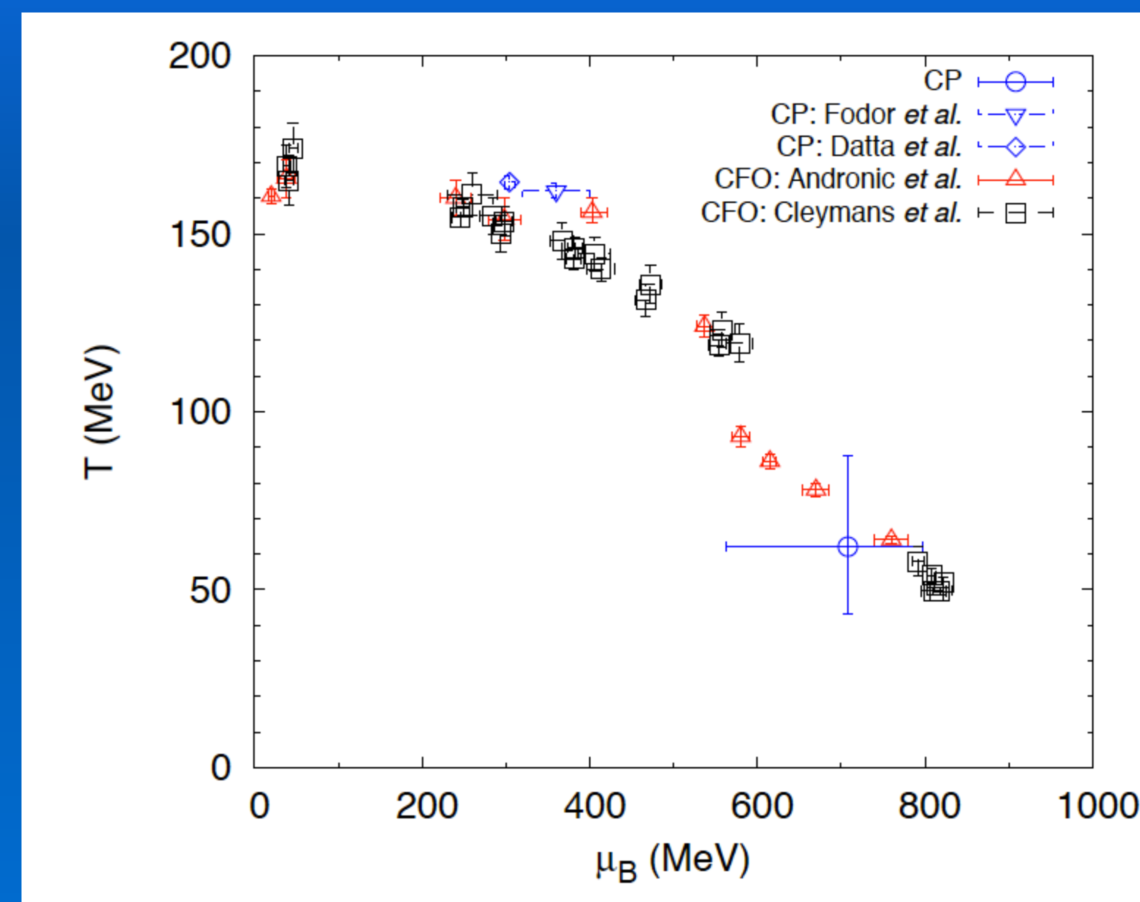

Critelli et al., arXiv:1706.00455 [nucl-th]

Samanta et al., arXiv:1709.04446 [hep-ph]

Criticality and CEP

Non-monotonicity and divergences are signal for critical behaviour, even at zero chemical potential.

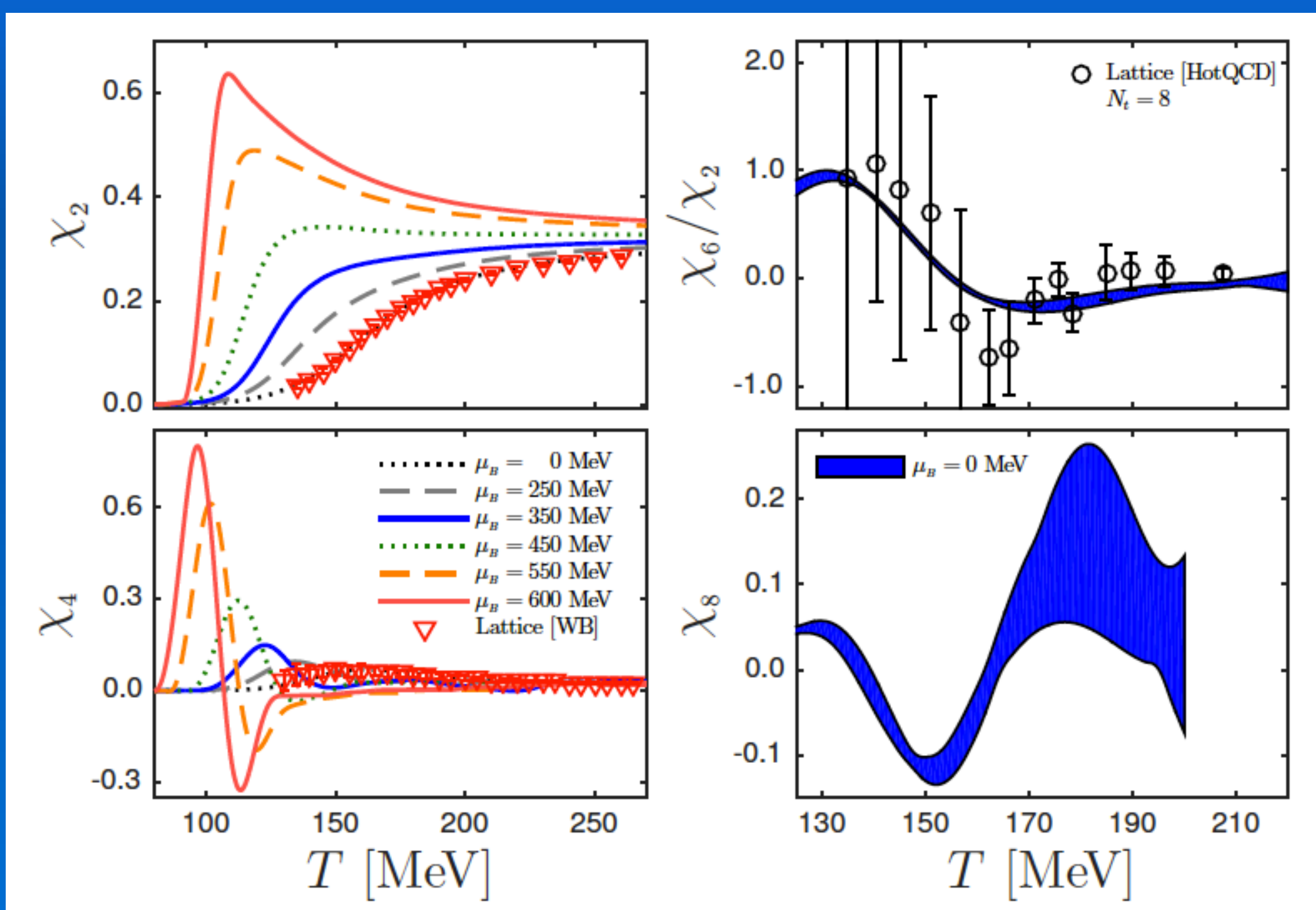

Critelli et al., arXiv:1706.00455 [nucl-th]

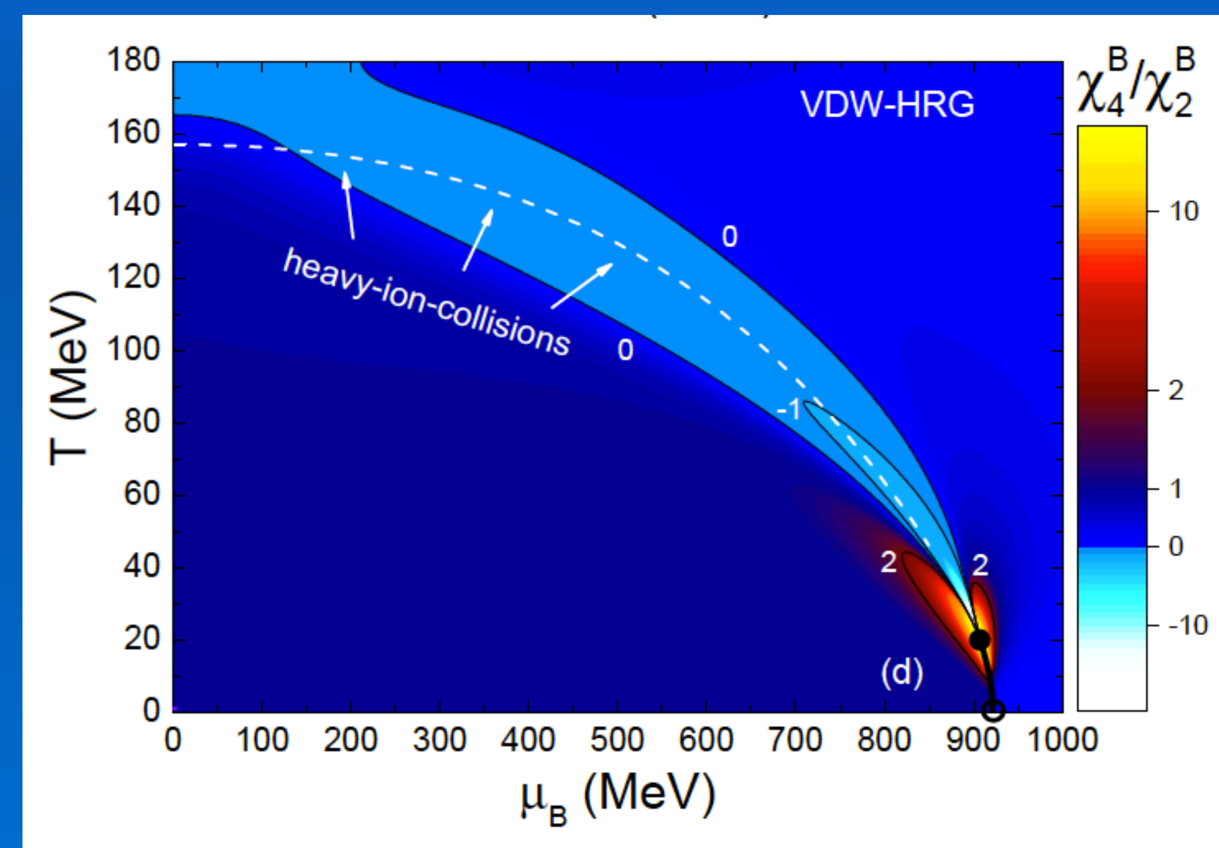

Vovchenko et al., Phys.Rev.Lett. 118 (2017) no.18, 182301

Fluctuations of charges

Lattice

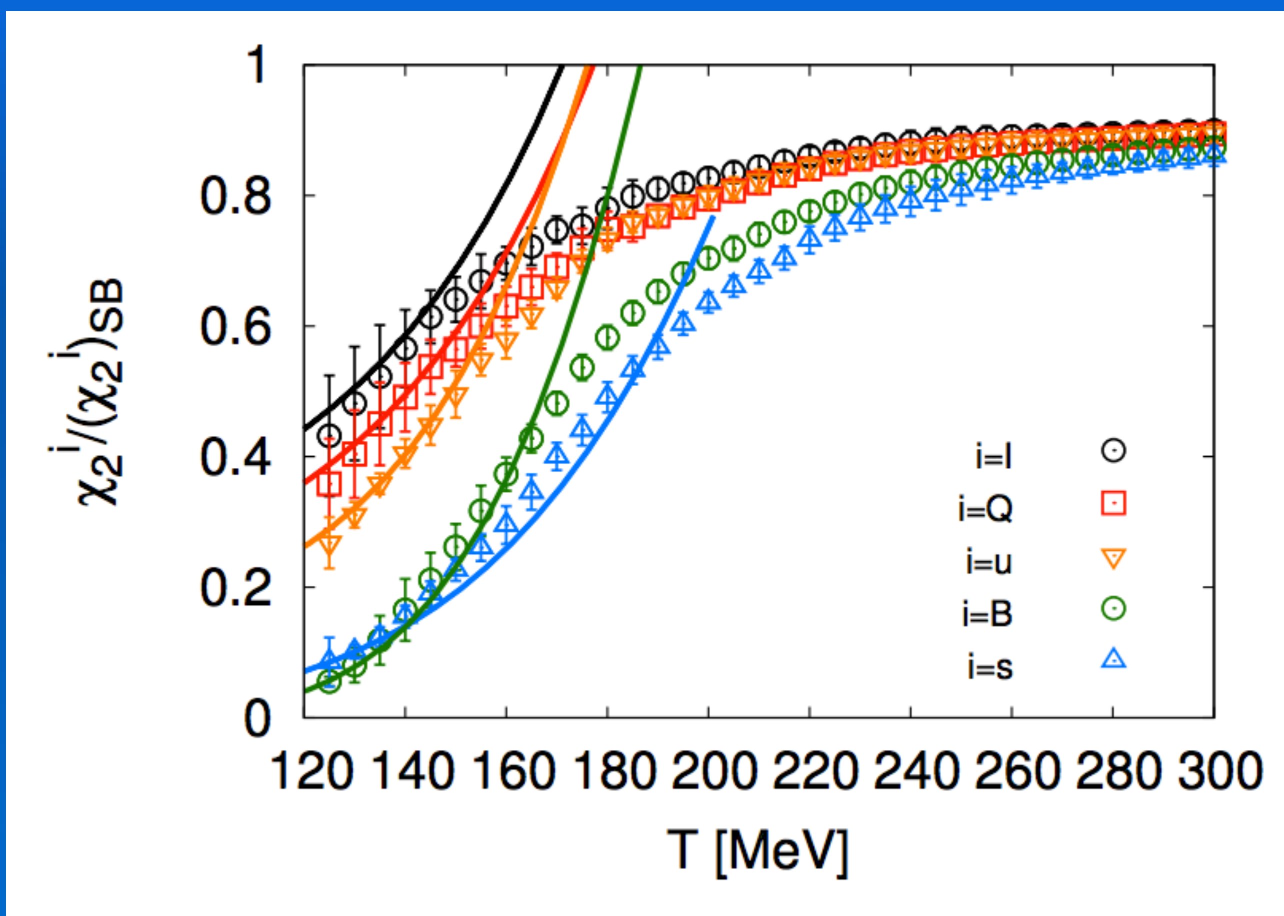

Borsanyi et al., JHEP 1201 (2012) 138

from yields

Experiment

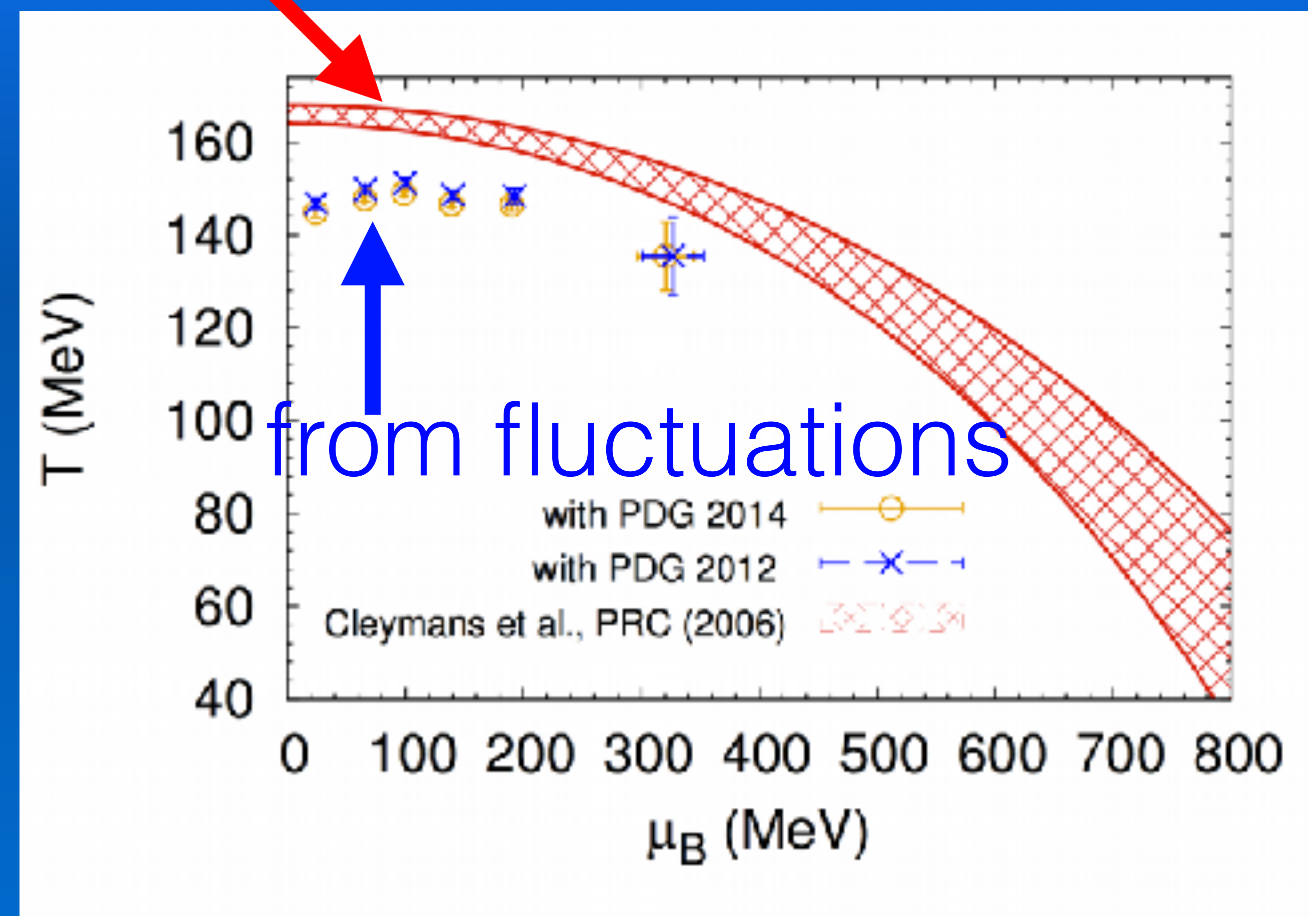

P.A. et al., Phys.Lett. B738 (2014) 305-310

The HRG model

A system of non-interacting resonances can describe most of the *attractive* interactions among hadrons.

$$\ln \mathcal{Z}(T,\{\mu_i\}) = \sum_{i \in Particles} (-1)^{B_i+1} \frac{d_i}{(2\pi^3)} \int d^3\vec{p} \ln \left[1 + (-1)^{B_i+1} e^{-(\sqrt{\vec{p}^2 + {m_i}^2} - \mu_i)/T}\right]$$

$$\mu_i = chemical\ potential$$

$$B_i = Baryon\ number$$

⋮

Here particles are assumed to be pointlike, with an infinite life-time, masses in vacuum, etc.

Hadronic spectrum

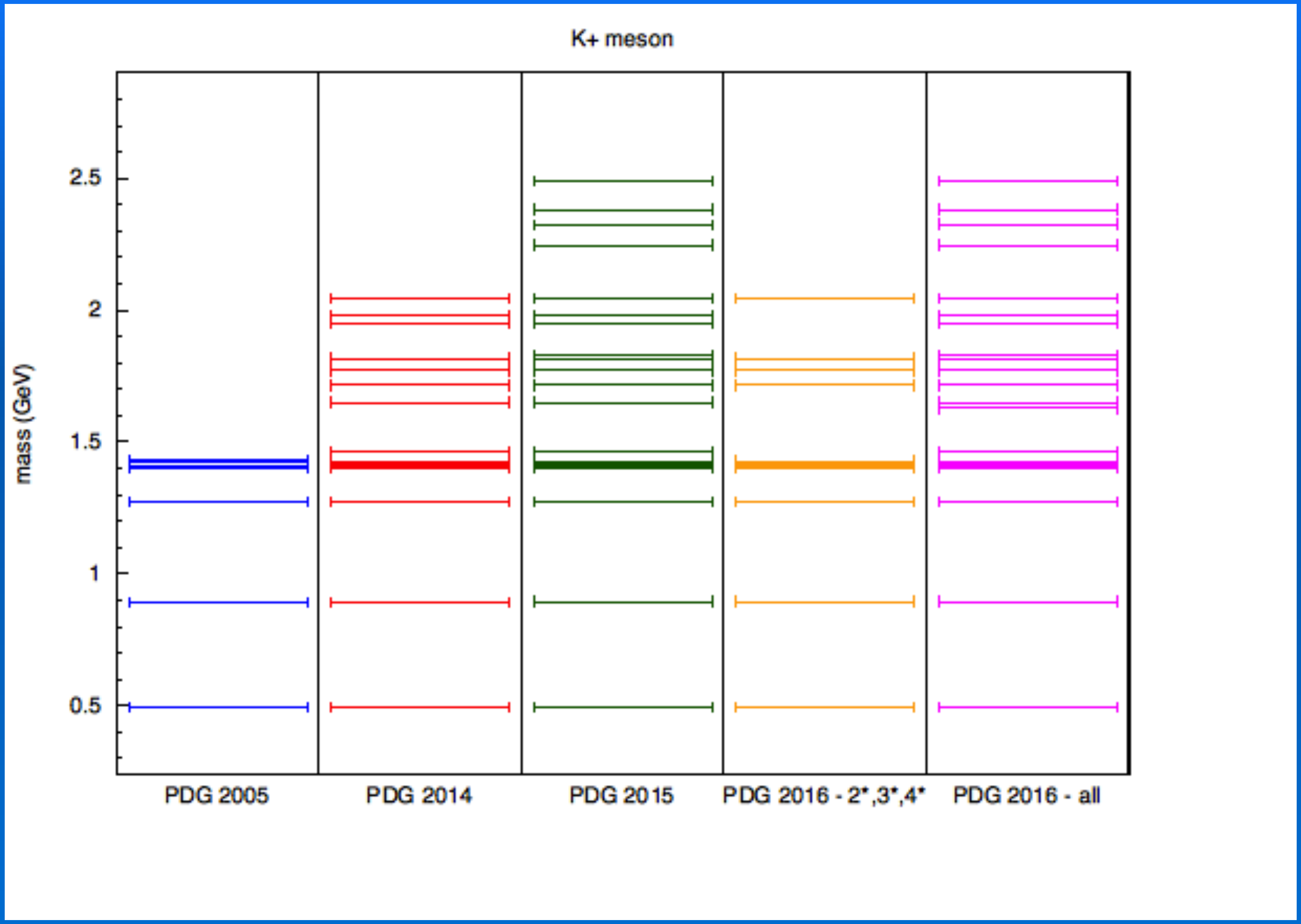

The strange sector is the one which got the largest and most relevant changes in recent years.

Hadronic spectrum

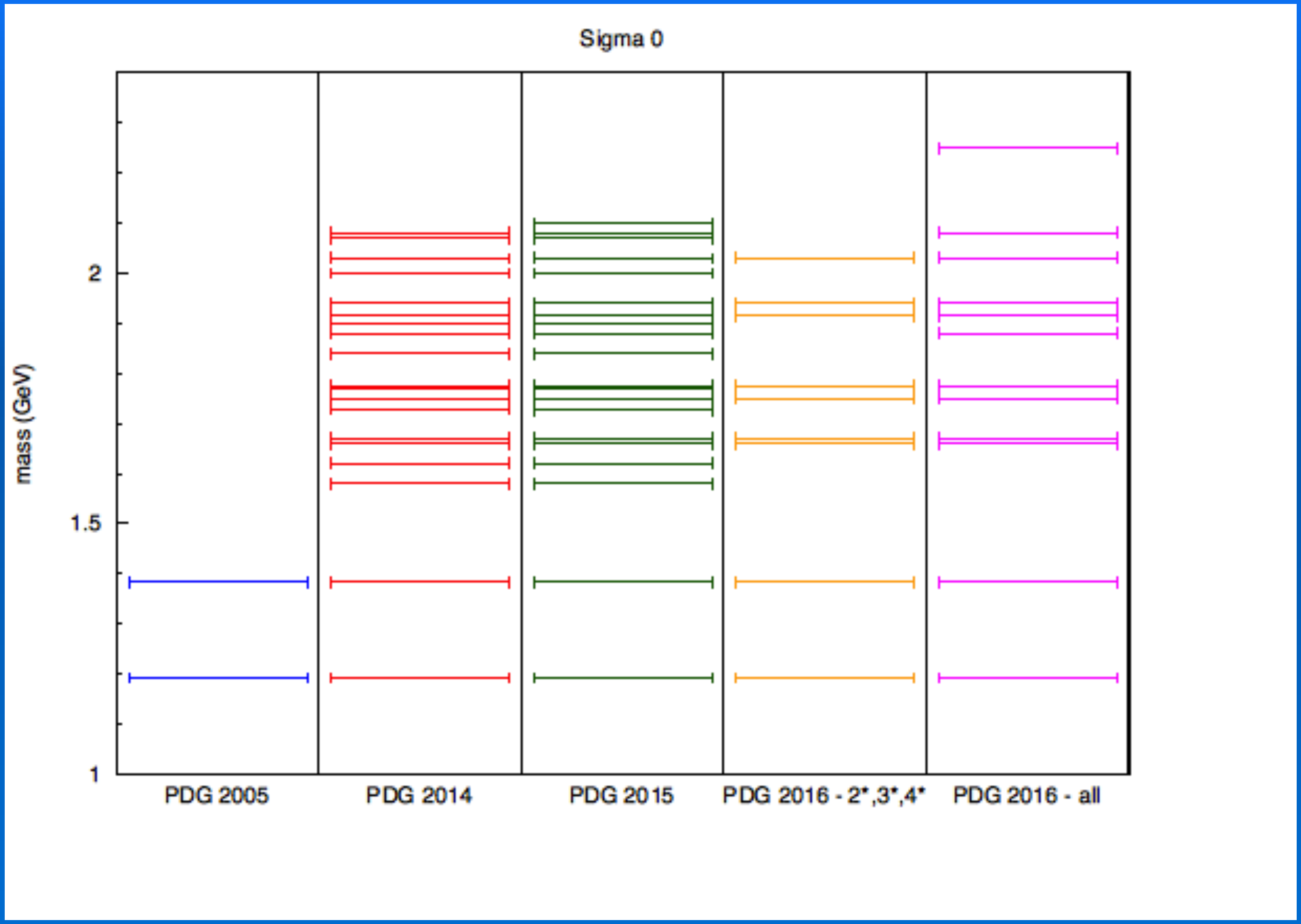

The strange sector is the one which got the largest and most relevant changes in recent years.

Hadronic spectrum

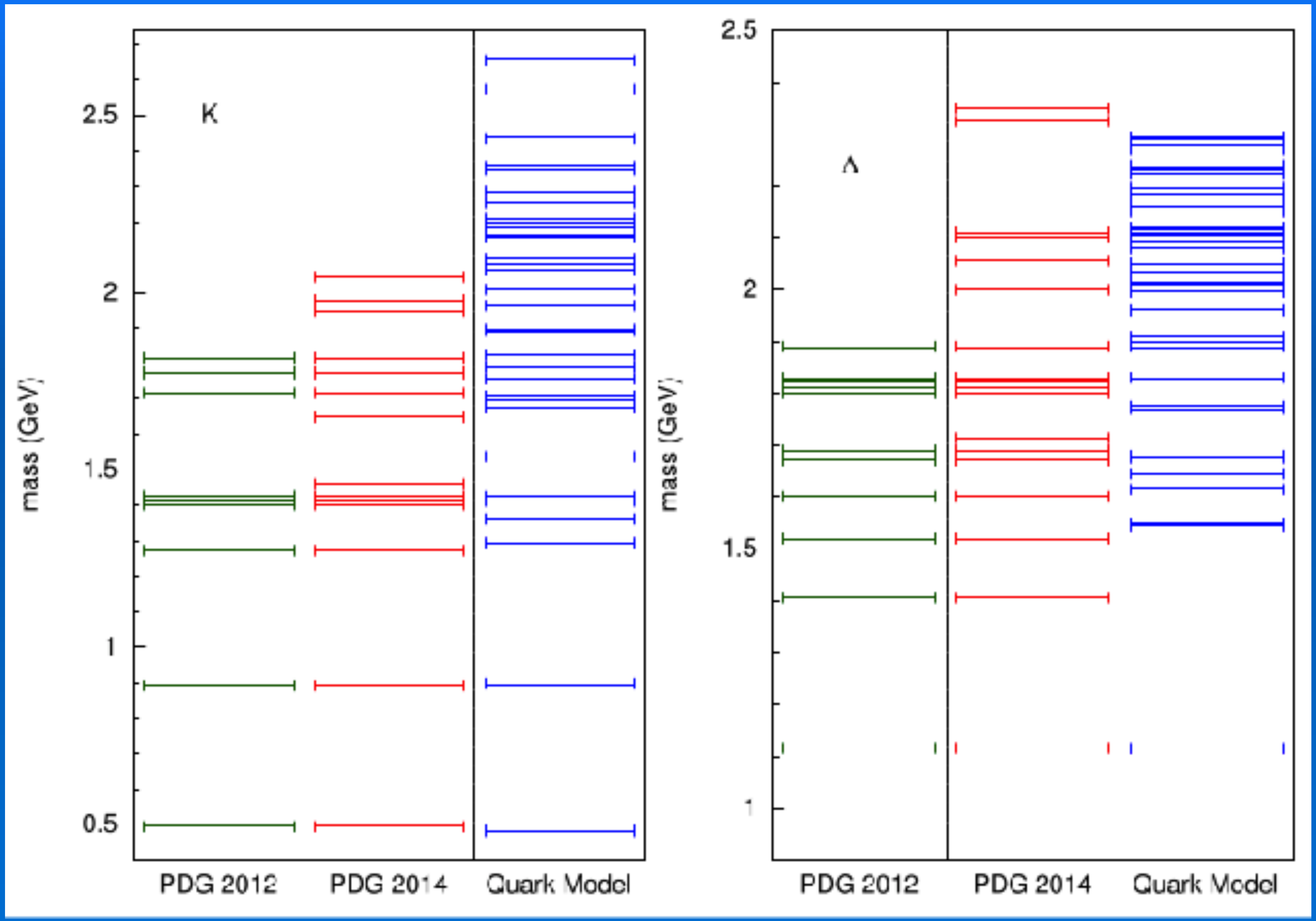

P.A. et al., Phys.Rev. D96 (2017) no.3, 034517

$\text{PDG} \simeq 600$

$\text{QM} \simeq 1500$

The *Quark Model* predicts a larger number of states with respect to the ones actually measured.

D. Ebert et al., Phys.Rev. D79 (2009) 114029
S. Capstick et al., Phys.Rev. D34 (1986) 2809

More strange baryons?

$$\left.\frac{\mu_S}{\mu_B}\right|_{LO} \simeq -\frac{\chi^{11}_{BS}}{\chi^2_S}$$

$$\frac{\chi^4_S}{\chi^2_S} \simeq \langle S^2 \rangle$$

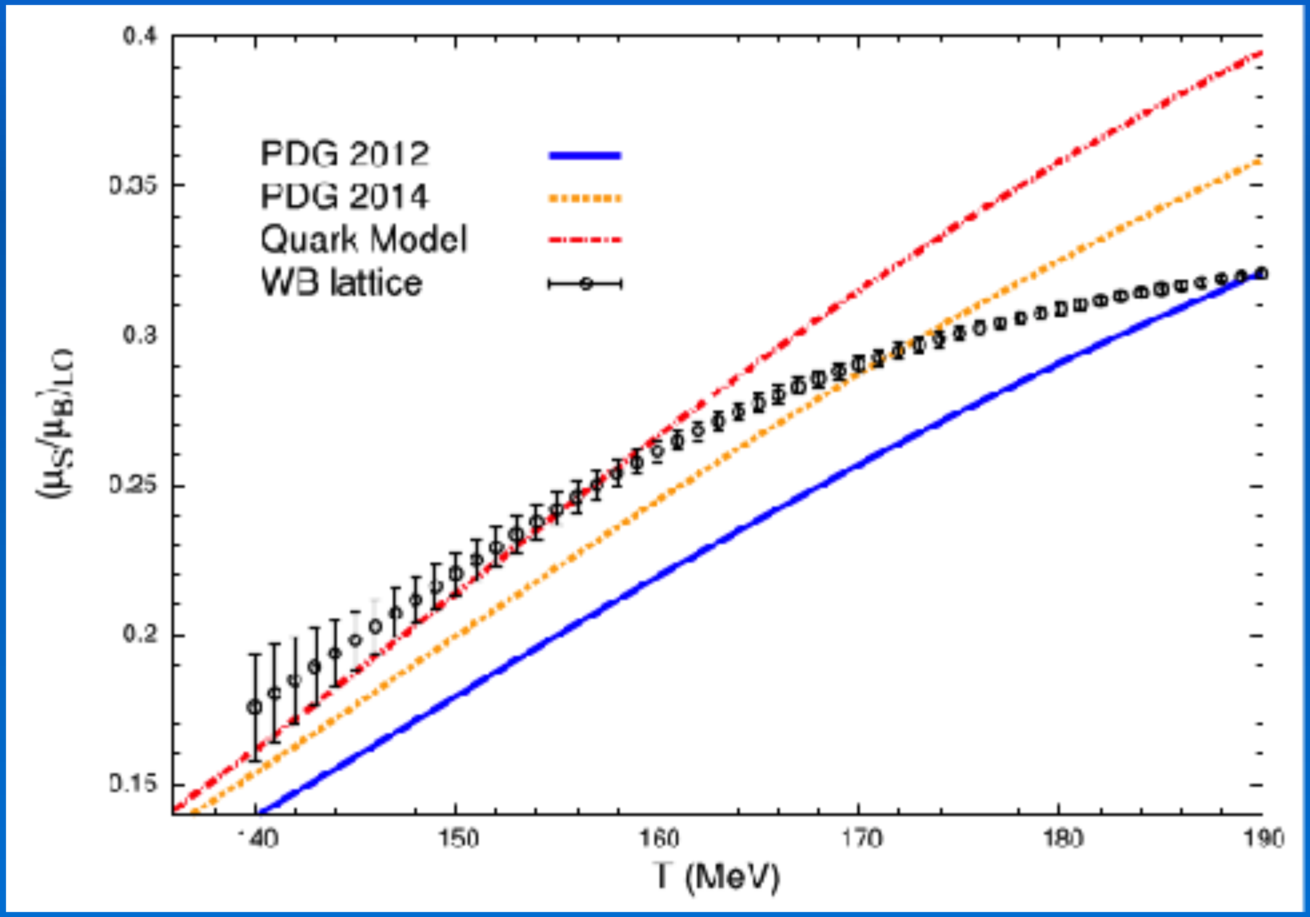

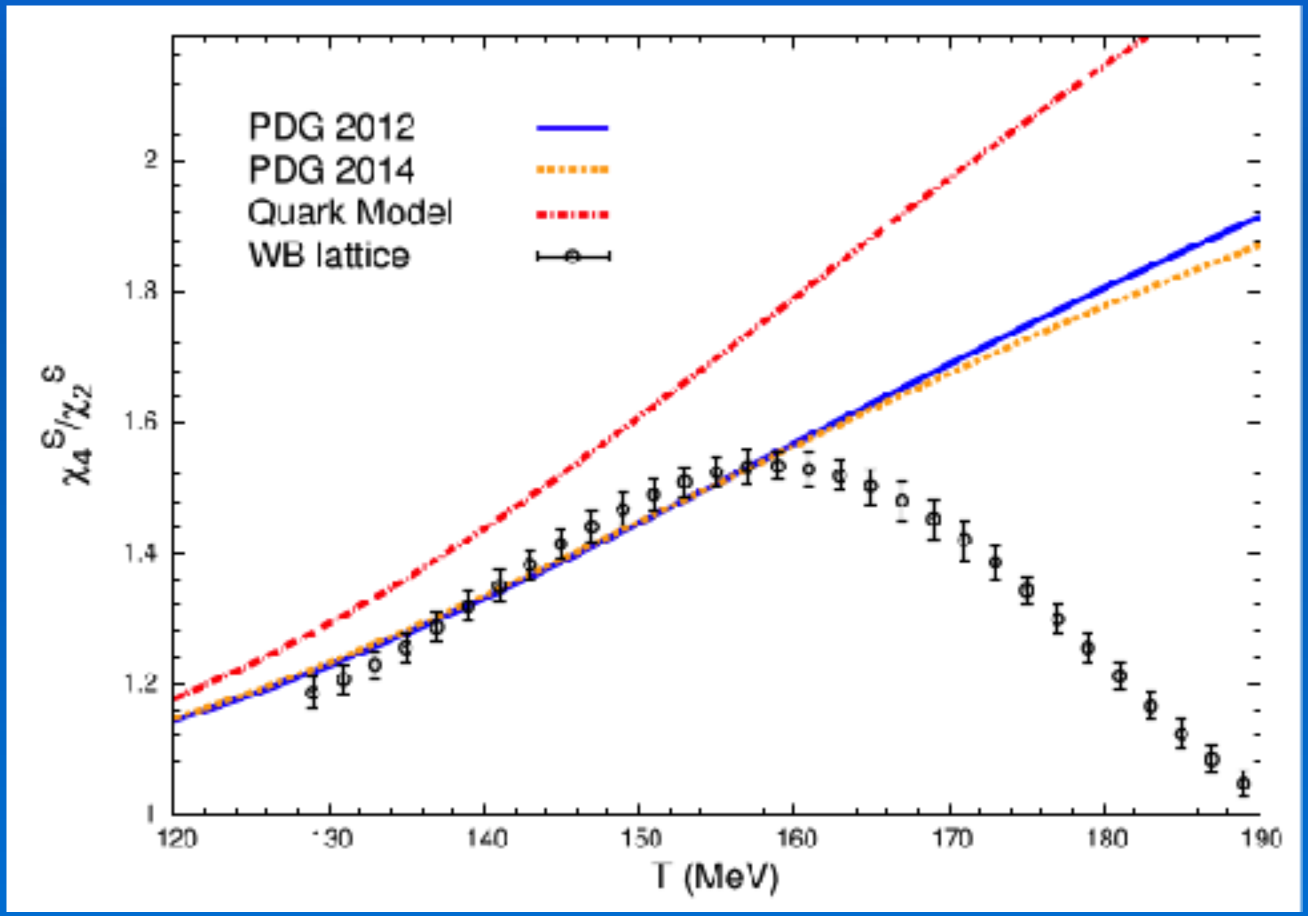

P.A. et al., Phys.Rev. D96 (2017) no.3, 034517
Bazavov et al., Phys.Rev.Lett. 113 (2014) no.7, 072001

Missing resonances in spectra

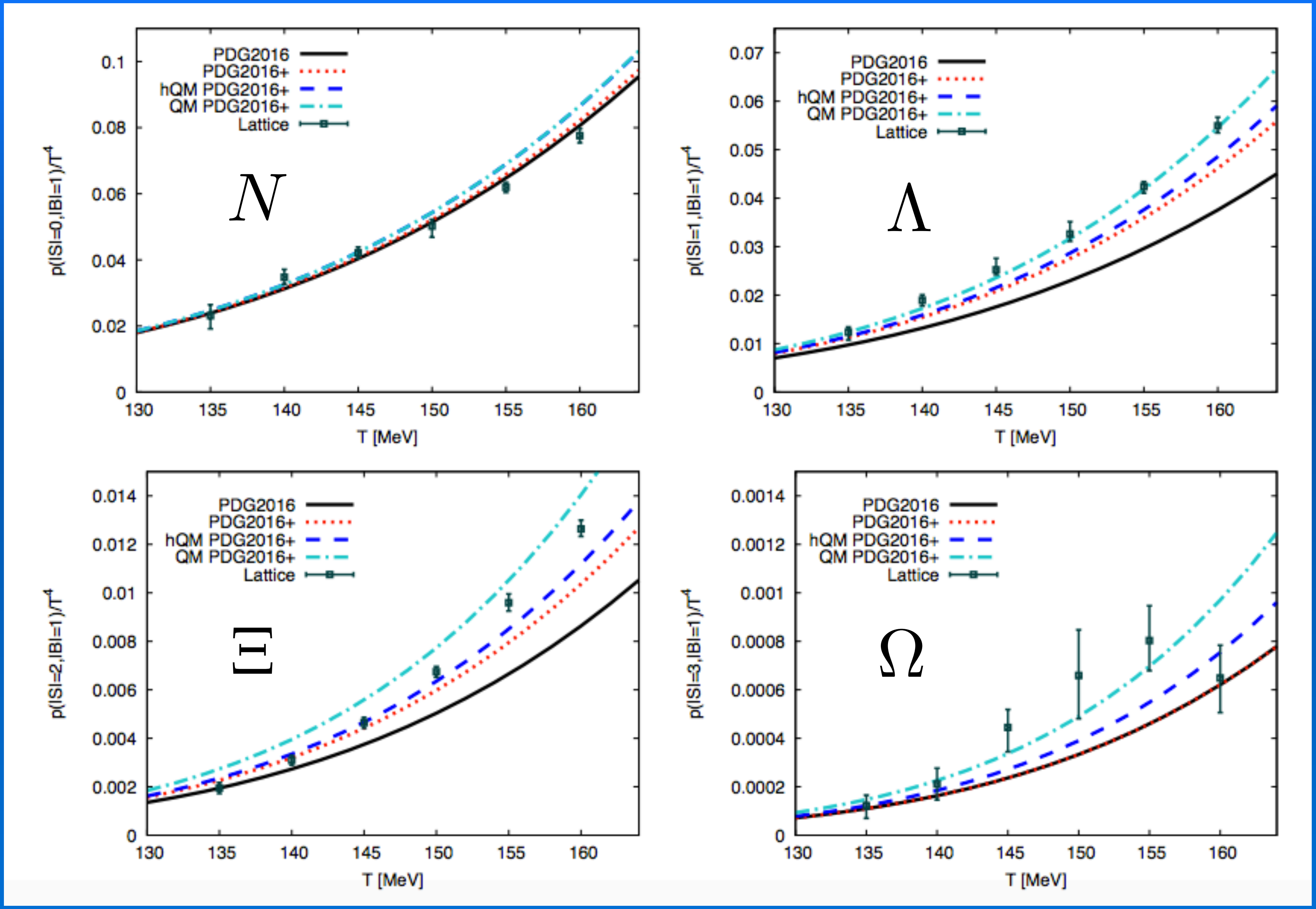

Particular combinations of fluctuations give selective informations on a specific hadronic sector.

P.A. et al., Phys.Rev. D96 (2017) no.3, 034517

Extra resonances on yields

ALICE@2.76 TeV

	T (MeV)	μ_B (MeV)	V (fm ^{3})	χ^2/N_{dof}
PDG05	156.2±2.2	5.8±7.2	5224.8±624.8	14.8/9≃1.6
PDG14	155.2±2.2	3.8±7	4663.1±590.3	20/9≃2.2
PDG17	147.6±1.8	4.9±6.9	6995.8±792.6	14.8/9≃1.6
QM	148.3±1.8	6.9±7.2	6182.7±710.4	11.4/9≃1.2

STAR@200 GeV

	T (MeV)	μ_B (MeV)	V (fm ^{3})	χ^2/N_{dof}
PDG05	160.6±1.9	26.9±9	2208.9±227.1	43.6/8≃5.4
PDG14	164.1±2.3	29.6±8.4	1492.1±187.8	14.1/8≃1.8
PDG17	156.5±2.0	25.8±7.9	2234.9±268.7	14/8≃1.8
QM	157.0±1.9	31.1±8.3	1934.9±232.6	7.4/8≃0.9

Missing resonances in spectra?

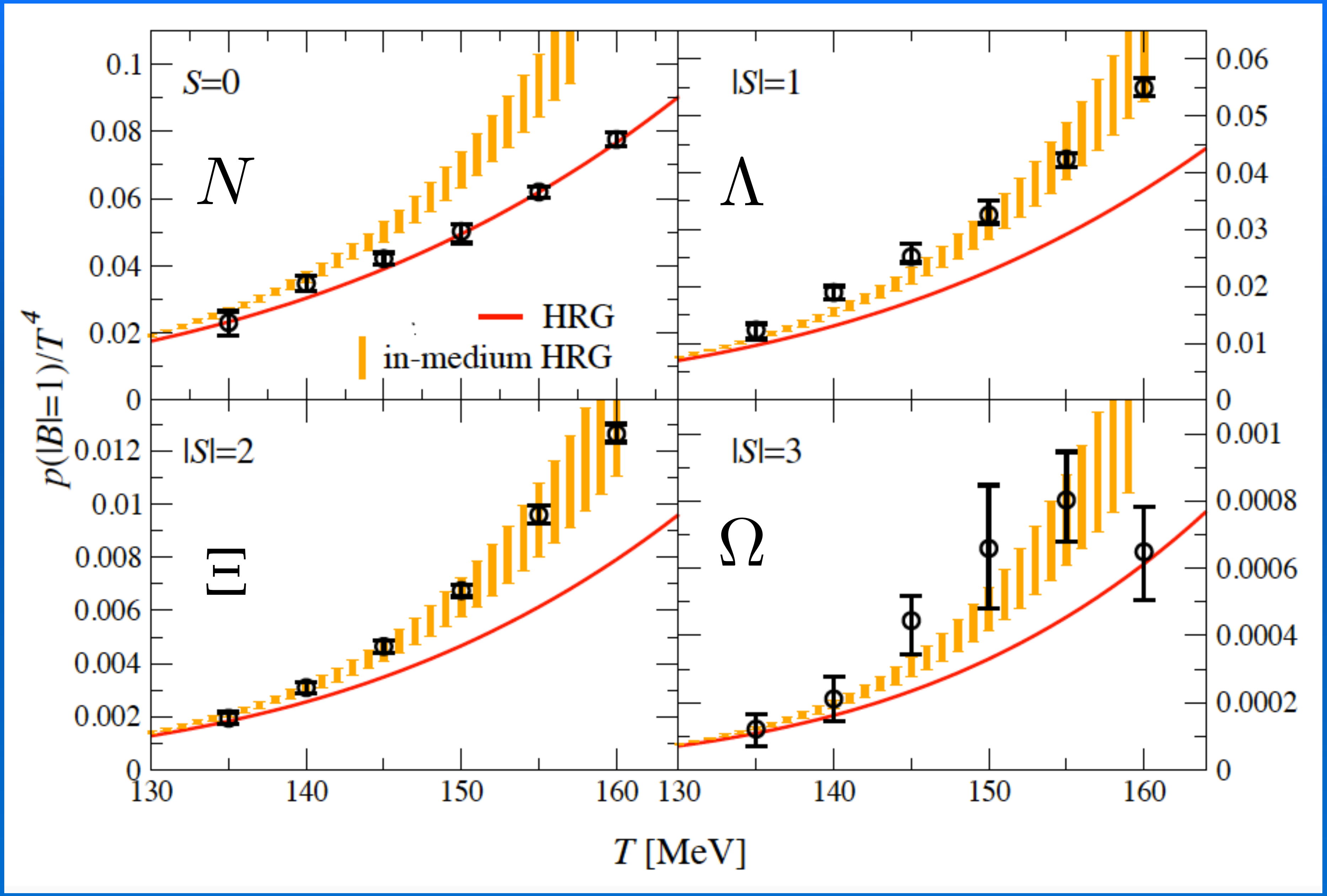

In-medium effects are relevant

Aarts, De Boni et al., arXiv:1710.00566 [hep-lat]

Phase shift vs HRG

Repulsive channels counteract interactive ones. In the case of the sigma meson they completely balance each other.

$$\ln \mathcal{Z} = \ln \mathcal{Z}_\pi + f_{IJ} \int_0^\infty dM \frac{d\delta_{IJ}}{\pi dM} \int \frac{d^3\vec{p}}{(2\pi)^3} \ln \left[1 - e^{-E_p/T}\right]^{-1}$$

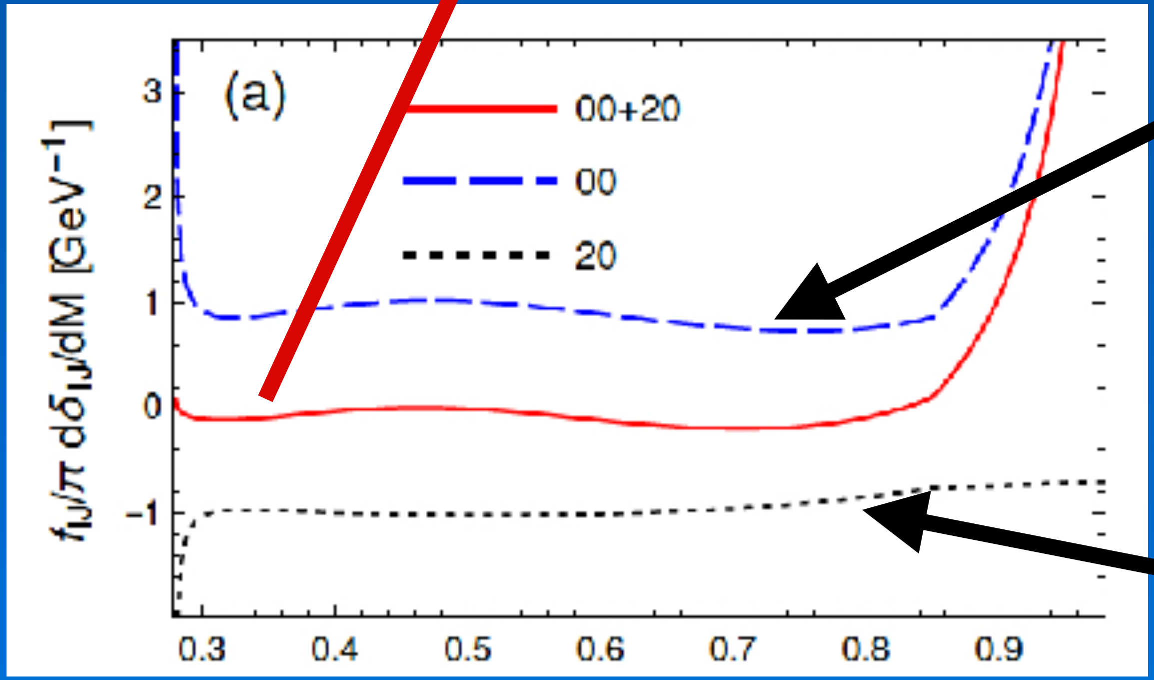

What is usually included in the HRG

The contribution from repulsive channel

Broniowski et al., Phys.Rev. C92 (2015) no.3, 034905

Phase shift vs HRG

The same applies partially for other states, BUT we need to have experimental data for the corresponding channels.

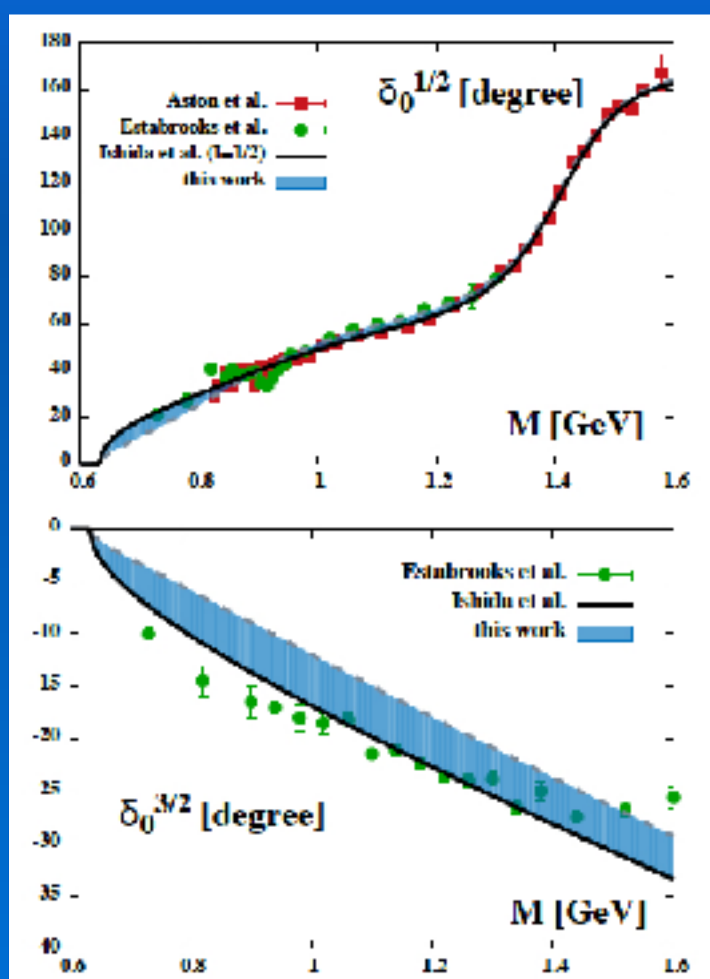

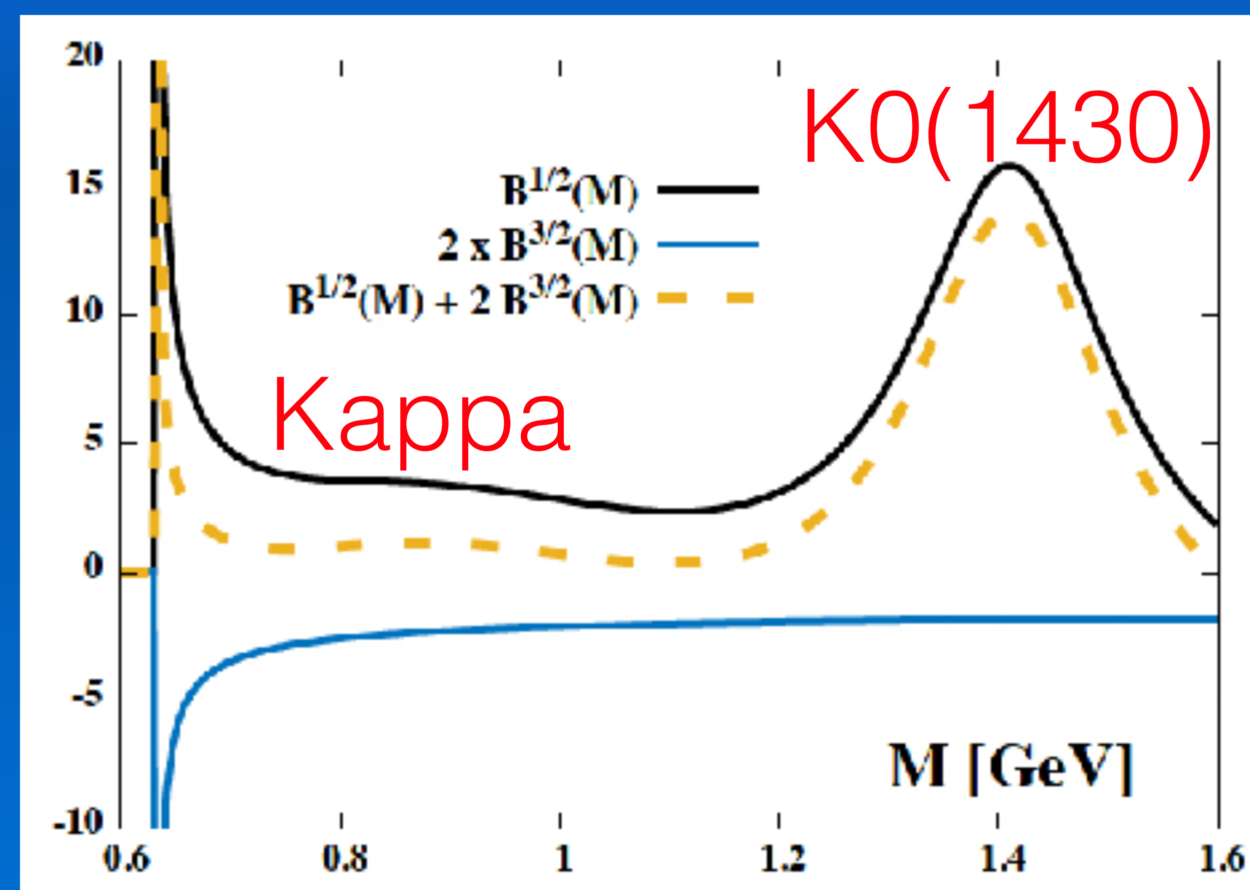

Pok Man Lo et al., Phys.Rev. D92 (2015) no.7, 074003

Phase shift vs HRG

NN phase shifts have been used to calculate BS susceptibilities.

$$b_2(T) = \frac{2T}{\pi^3}\int_0^\infty dE\left(\frac{ME}{2}+M^2\right)K_2\left(2\beta\sqrt{\frac{ME}{2}+M^2}\right)\frac{1}{4i}\mathrm{Tr}\left[S^\dagger\frac{dS}{dE}-\frac{dS^\dagger}{dE}S\right]$$

These combinations are zero in the standards HRG!!!!

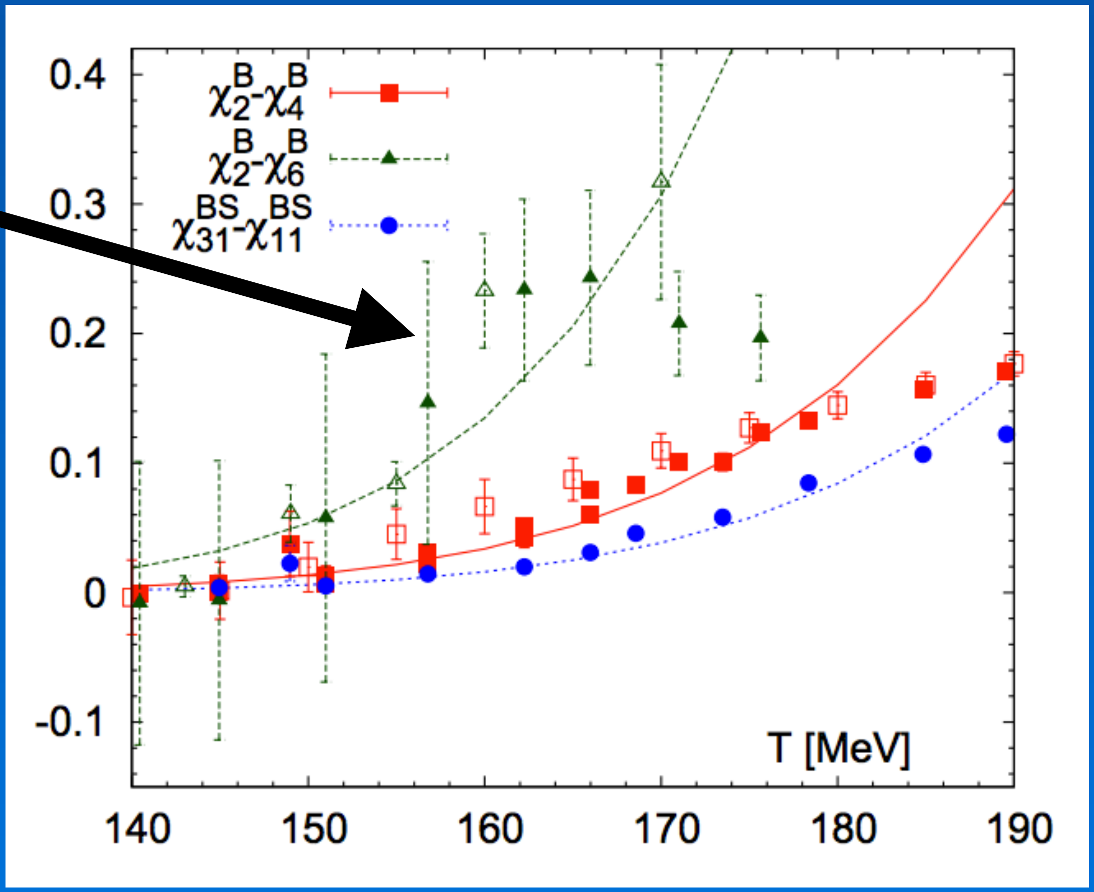

These effects are entirely due to hadronic interactions!!!

P. Huovinen et al., 1708.00879 [hep-ph]

EV effects into the HRG

Repulsive interactions can be easily implemented in the HRG by means of hard spheres. This results into a shifted chemical potential.

$$p(T,\vec{\mu}) = \sum_j p_j^{id}(T,\mu_j)$$

$$p(T,\vec{\mu}) = \sum_j p_j^{id}(T,\mu_j^*)$$

$$\mu_j^* = \mu_j - v_j p(T,\vec{\mu})$$

$$v_j = \frac{16}{3}\pi r_j^3$$

+

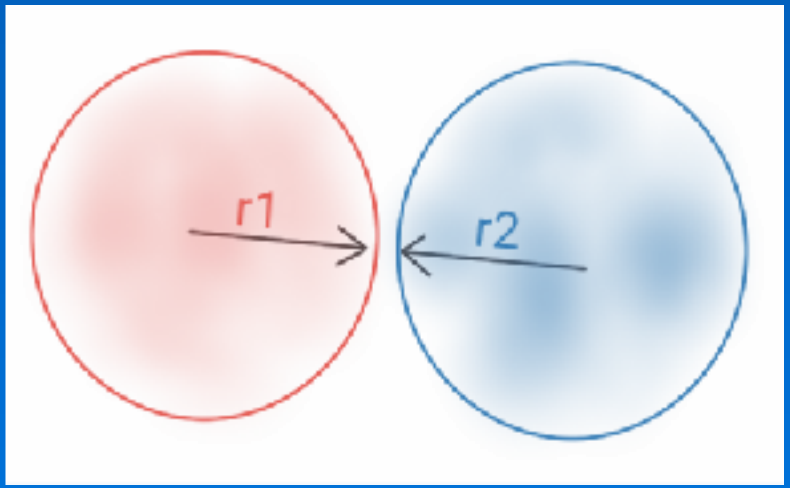

D.H. Rischke et al., Z.Phys. C51 (1991) 485-490

M. Albright et al., Phys.Rev. C90 (2014) no.2, 024915

EV effects into the HRG

Repulsive interactions can be easily implemented in the HRG by means of hard spheres. This results into a shifted chemical potential.

$$n_B(T,\vec{\mu}) = \sum_i \frac{B_i n_i^{id}(T,\mu_i^*)}{1+\sum_j v_j n_j^{id}(T,\mu_j^*)}$$

$$p(T,\vec{\mu}) = \sum_j p_j^{id}(T,\mu_j^*)$$

$$\mu_j^* = \mu_j - v_j p(T,\vec{\mu})$$

$$v_j = \frac{16}{3}\pi r_j^3$$

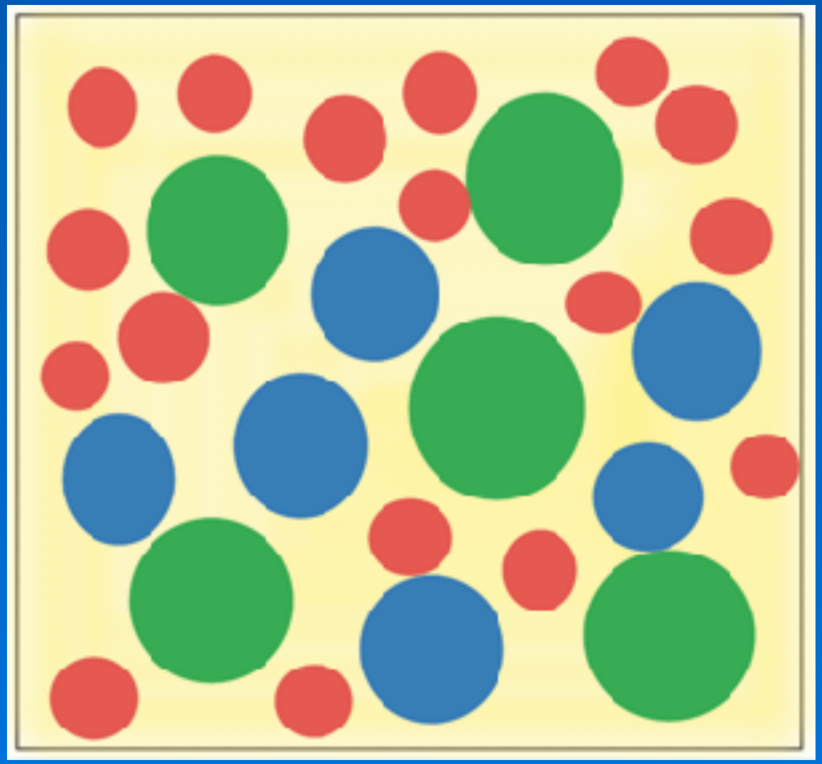

D.H. Rischke et al., Z.Phys. C51 (1991) 485-490

M. Albright et al., Phys.Rev. C90 (2014) no.2, 024915

EV effects into the HRG

Repulsive interactions can be easily implemented in the HRG by means of hard spheres. This results into a shifted chemical potential.

$$n_B(T,\vec{\mu}) = \sum_i \frac{B_i n_i^{id}(T,\mu_i^*)}{1+\sum_j v_j n_j^{id}(T,\mu_j^*)}$$

$$p(T,\vec{\mu}) = \sum_j p_j^{id}(T,\mu_j^*)$$

$$\mu_j^* = \mu_j - v_j p(T,\vec{\mu})$$

$$v_j = \frac{16}{3}\pi r_j^3$$

$$fixed : v_j = v \;\forall\; j$$

$$direct : v_j \propto m_j$$

$$inverse : v_j \propto 1/m_j$$

D.H. Rischke et al., Z.Phys. C51 (1991) 485-490

M. Albright et al., Phys.Rev. C90 (2014) no.2, 024915

EV: Pure gauge

Consistency between SU2 and SU3!

	r (fm)	Δr (fm)	χ^2
point like	0	0	11.25
fixed	0.69	0.114	0.917
direct	0.518	0.095	1.95
inverse	0.861	0.147	0.45

	r (fm)	Δr (fm)	χ^2
point like	0	0	54.73
fixed	0.717	0.047	2.07
direct	0.526	0.036	3.12
inverse	0.907	0.062	2.05

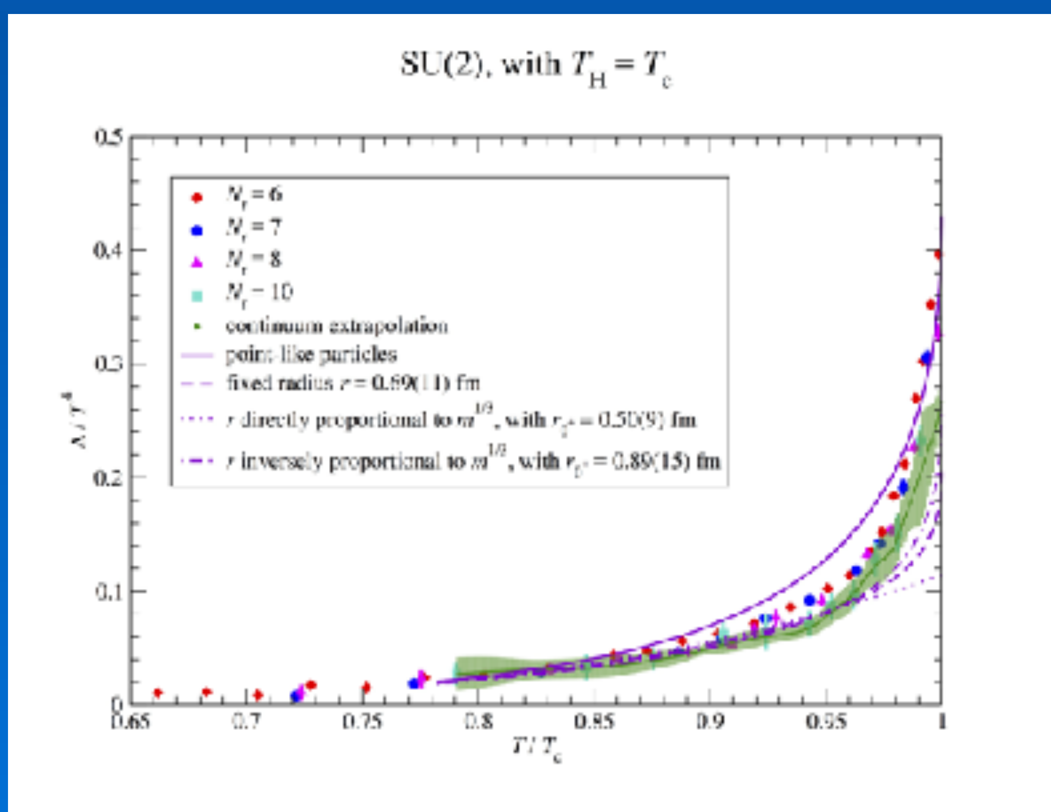

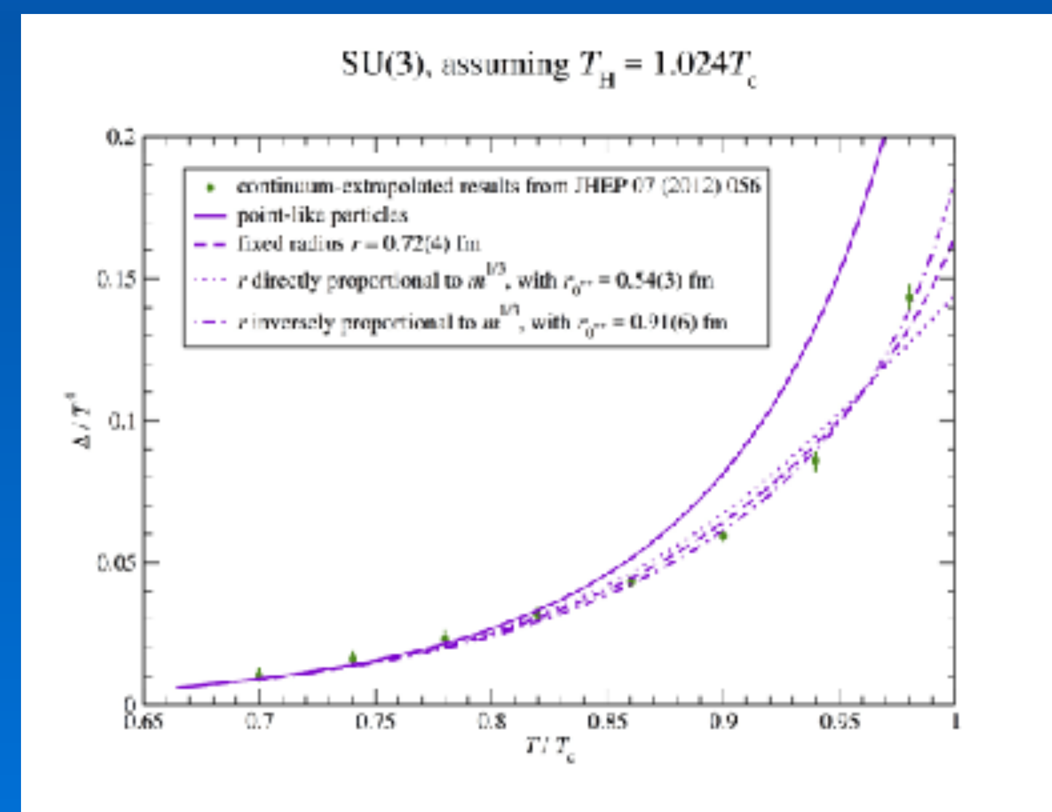

P.A. et al., Phys.Rev. D95 (2017) no.9, 094511

EV + QM: fit to QCD

observables involved in the calculation of χ^2:

- thermodynamic: P/T^2, Δ/T^4;
- light: χ_4/χ_2 net-B, χ_4/χ_2 net-l, χ_{ud};
- strange: χ_4/χ_2 net-S, χ_{us}, μ_S/μ_B LO, χ_2^S .

$$T_{min} = 110 \ \text{(MeV)}$$
$$T_{max} = 164 \ \text{(MeV)}$$

number of lattice points = 111

	PDG05	PDG14	PDG17	QM
χ^2/N_{dof}	49.645	10.094	9.331	16.312

More strange baryons →

EV + QM: fit to QCD

observables involved in the calculation of χ^2:

- thermodynamic: P/T^2, Δ/T^4;
- light: χ_4/χ_2 net-B, χ_4/χ_2 net-l, χ_{ud};
- strange: χ_4/χ_2 net-S, χ_{us}, μ_S/μ_B LO, χ_2^S .

$T_{min} = 110$ (MeV)

$T_{max} = 164$ (MeV)

number of lattice points = 111

	PDG05	PDG14	PDG17	QM
χ^2/N_{dof}	49.645	10.094	9.331	16.312

More strange baryons →

EV + QM: fit to QCD

I perform a fit to the lattice data, allowing light and strange particles to have a different behaviour, within different EV schemes.

		Fixed	Fixed
	χ^2/N_{dof}	r_p (fm)	r_Λ (fm)
PDG05	44.3	0.446 ±0.115	0.173 ±0.133
PDG14	5.723	0.389 ±0.101	0.173 ±0.1
PDG17	4.28	0.383 ±0.1	0.217 ±0.066
QM	6.263	0.351 ±0.099	0.274 ±0.044

EV + QM: fit to QCD

I perform a fit to the lattice data, allowing light and strange particles to have a different behaviour, within different EV schemes.

		Direct	Inverse
	χ^2/N_{dof}	r_p (fm)	r_Λ (fm)
PDG05	40.632	0.487 ±0.157	0.249 ±0.052
PDG14	3.717	0.404 ±0.099	0.171 ±0.063
PDG17	2.26	0.391 ±0.092	0.192 ±0.051
QM	8.585	0.353 ±0.078	0.201 ±0.043

EV + QM: fit to QCD

I perform a fit to the lattice data, allowing light and strange particles to have a different behaviour, within different EV schemes.

		Direct	Direct
	χ^2/N_{dof}	r_p (fm)	r_Λ (fm)
PDG05	45.48	0.394 ±0.093	0.004 ±0.432
PDG14	4.719	0.375 ±0.081	0.016 ±0.508
PDG17	3.595	0.373 ±0.085	0.172 ±0.073
QM	1.714	0.38 ±0.092	0.266 ±0.034

EV + QM: fit to QCD

The use of multiple parameters does not drastically improve the quality of the fit, but underlines an interesting systematic difference between PDG lists and the QM one.

		Fixed	Fixed	Fixed	Fixed
	χ^2/N_{dof}	r_π (fm)	r_K (fm)	r_p (fm)	r_Λ (fm)
PDG05	15.632	0.757 $\pm$0.093	0.515 $\pm$0.049	0.656 $\pm$0.114	0.006 $\pm$0.73
PDG14	2.611	0.208 $\pm$0.279	0.221 $\pm$0.059	0.446 $\pm$0.102	0.007 $\pm$0.486
PDG17	1.721	0.161 $\pm$0.399	0.224 $\pm$0.058	0.435 $\pm$0.096	0.113 $\pm$0.221
QM	1.257	0.171 $\pm$0.339	0.214 $\pm$0.063	0.42 $\pm$0.095	0.285 $\pm$0.038

EV + QM: fit to QCD

The use of multiple parameters does not drastically improve the quality of the fit, but underlines an interesting systematic difference between PDG lists and the QM one.

Experimental estimates

(fm)	$\pi^{\pm}$	$K^{\pm}$	p	Σ^{-}
$\sqrt{\langle r_E^2 \rangle}$	0.672±0.008	0.569±0.031	0.8751±0.0061	0.78±0.10
$\sqrt{\langle r_M^2 \rangle}$	NA	NA	0.78±0.04	NA

EV + QM: strange obs.

$$\left.\frac{\mu_S}{\mu_B}\right|_{LO} \simeq -\frac{\chi^{11}_{BS}}{\chi^2_S}$$

$$\frac{\chi^4_S}{\chi^2_S} \simeq \langle S^2 \rangle$$

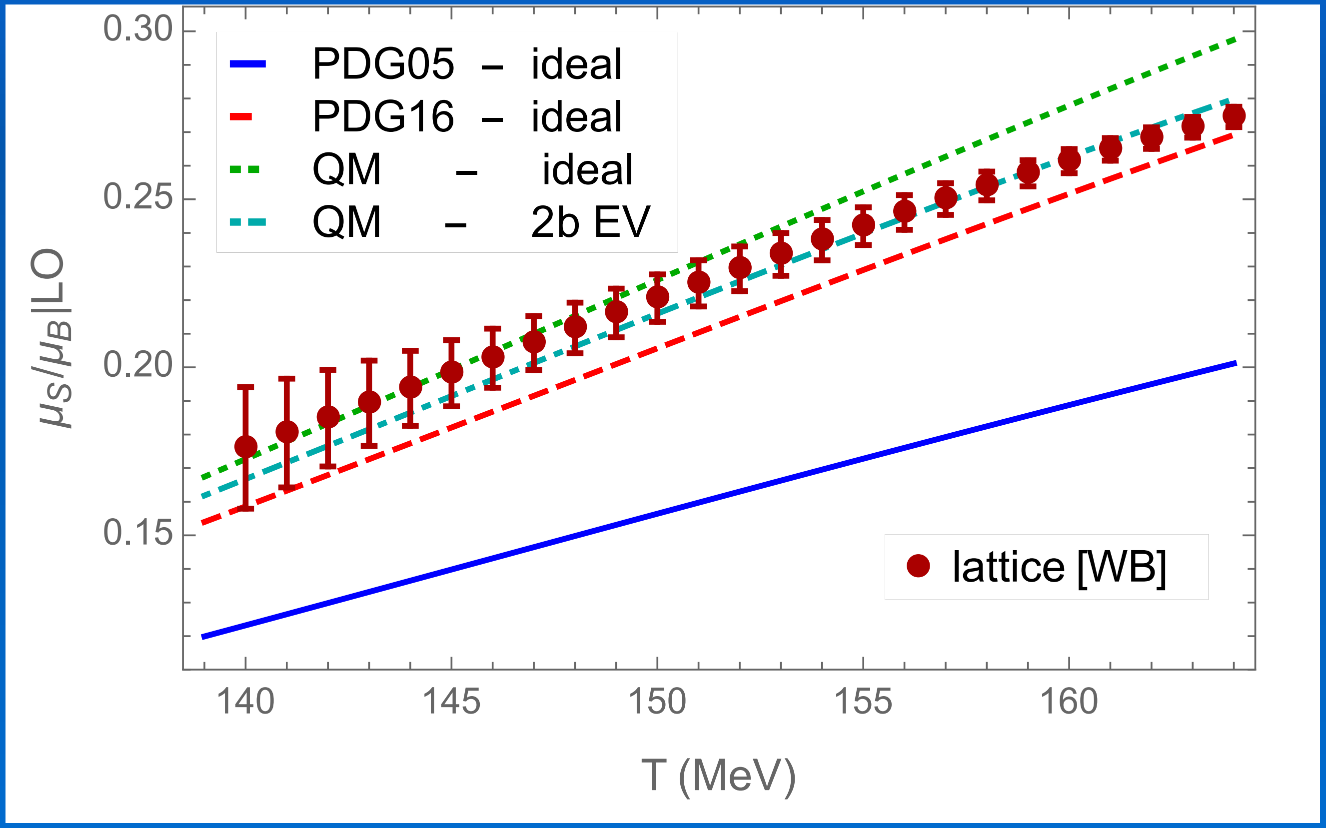

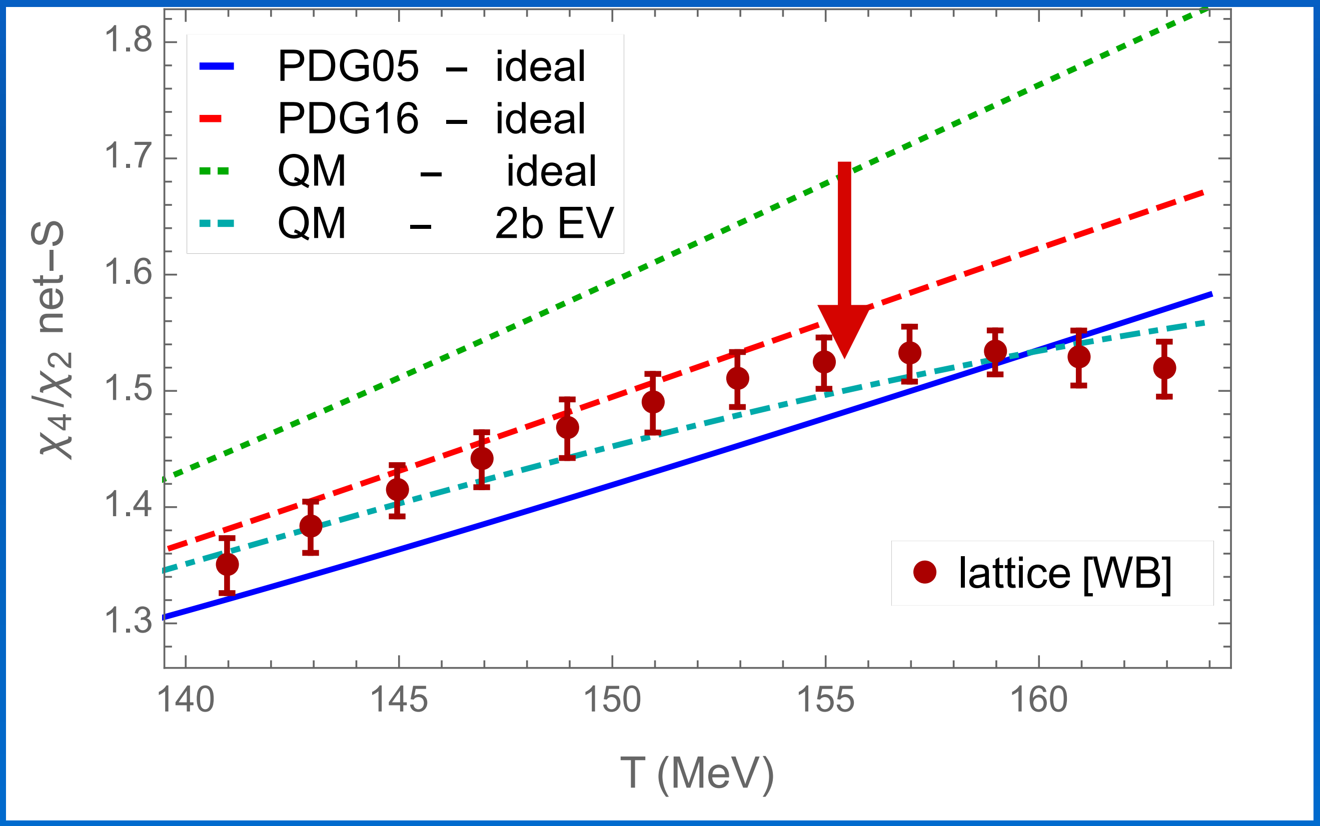

EV + QM: EoS

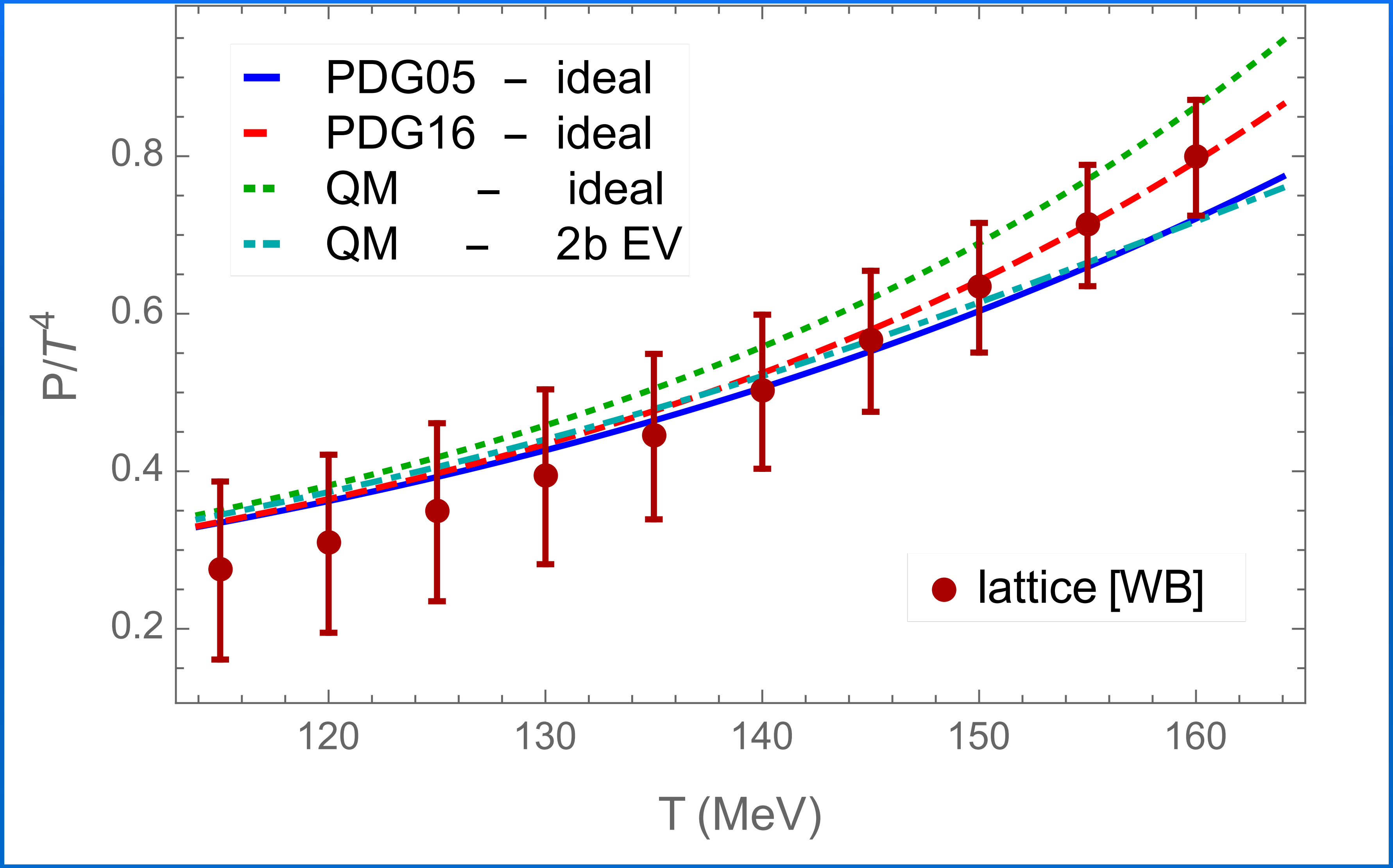
PDG05 – ideal
PDG16 – ideal
QM – ideal
QM – 2b EV
lattice [WB]
P/T^4
0.2
0.4
0.6
0.8
120
130
140
150
160
T (MeV)

EV + QM: light obs.

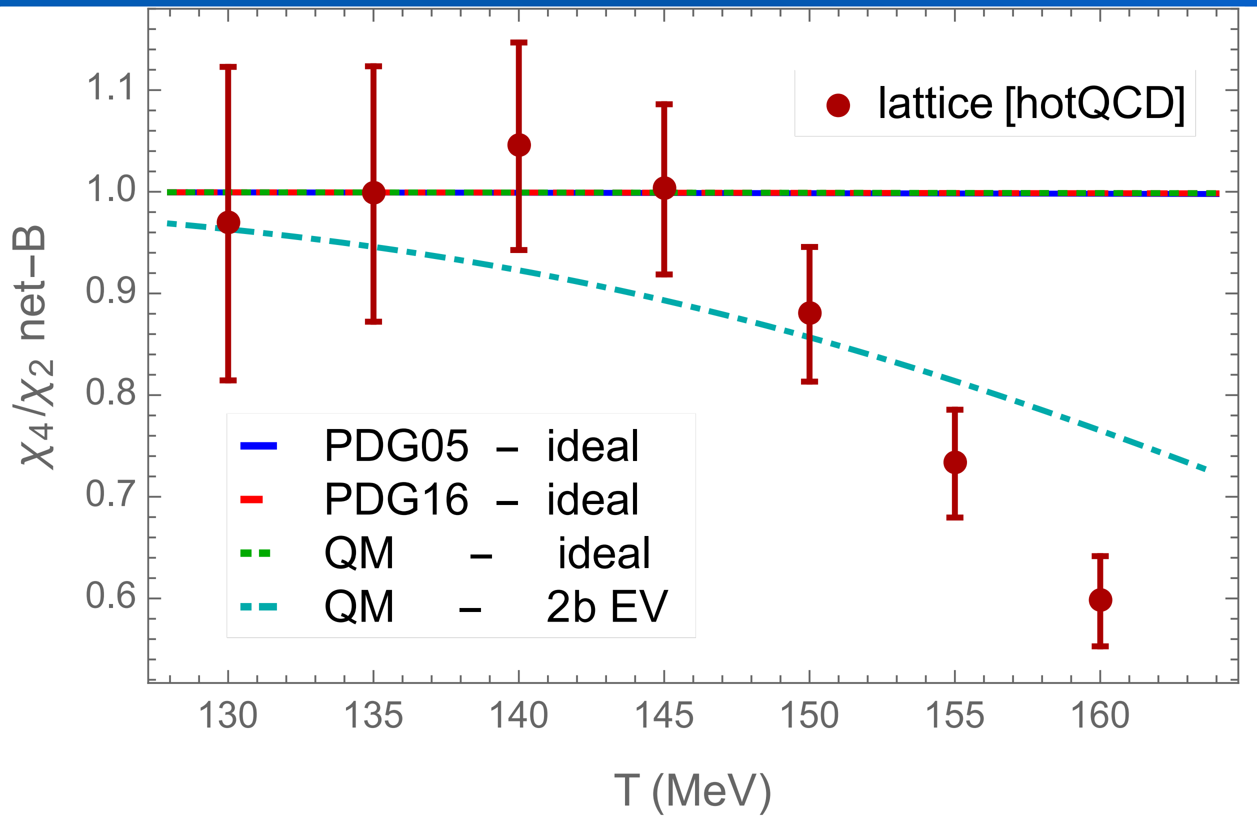

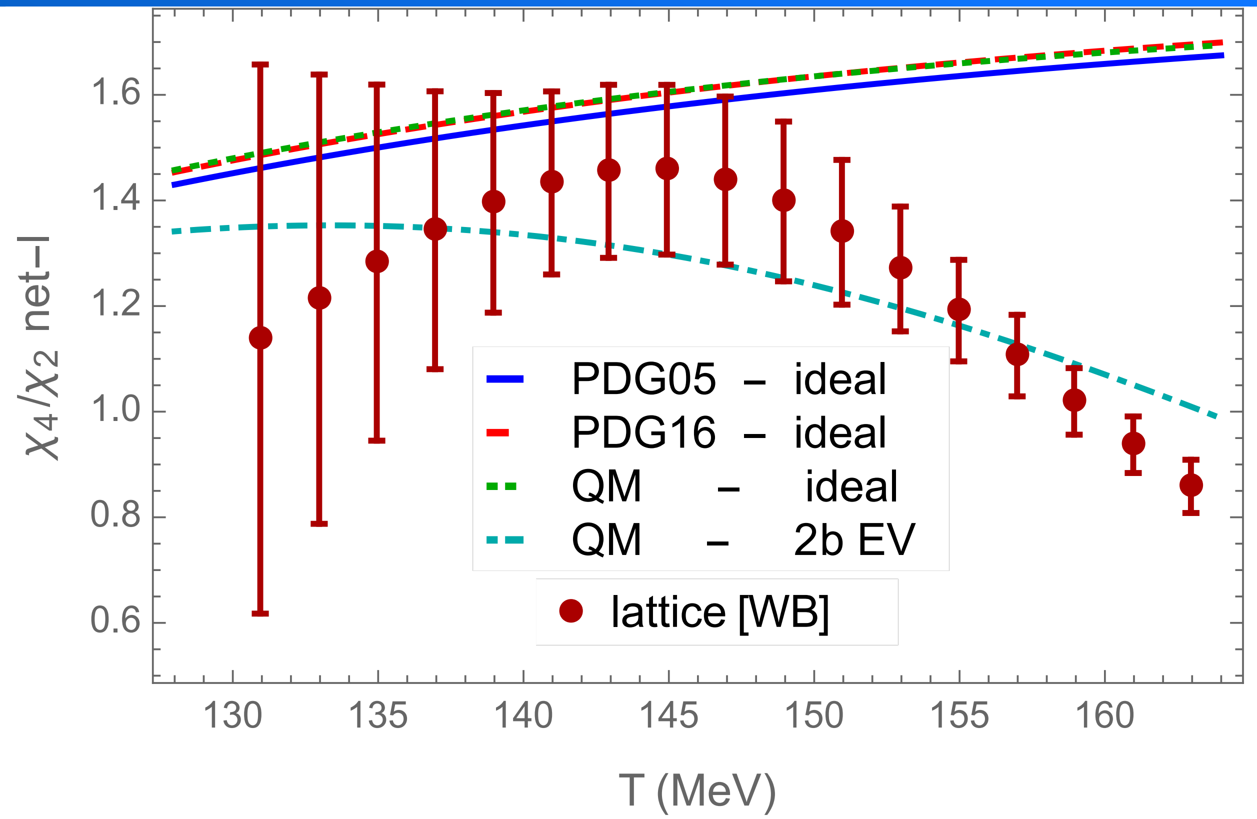

EV + QM: no-fitted obs.

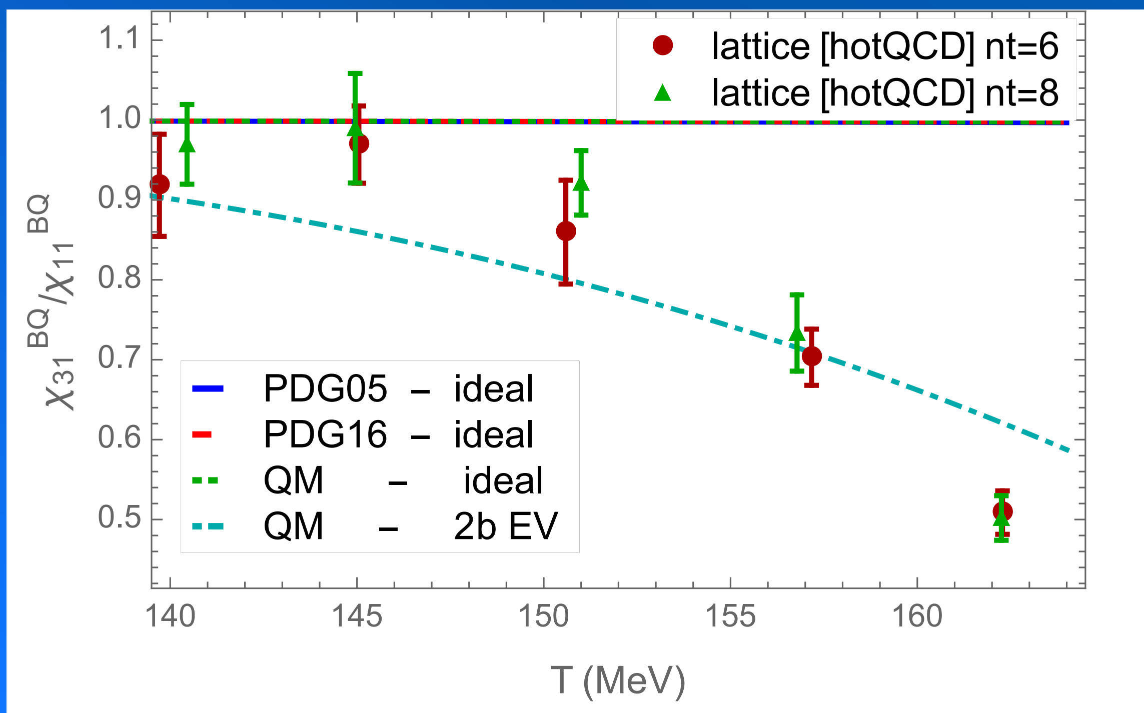

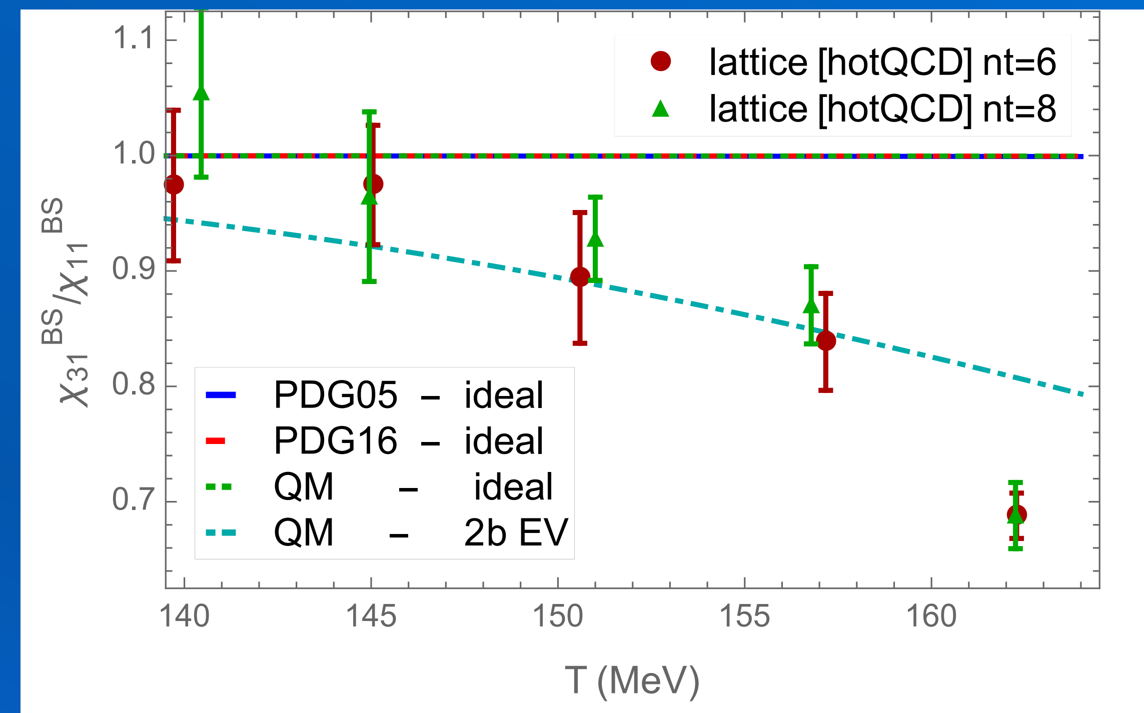

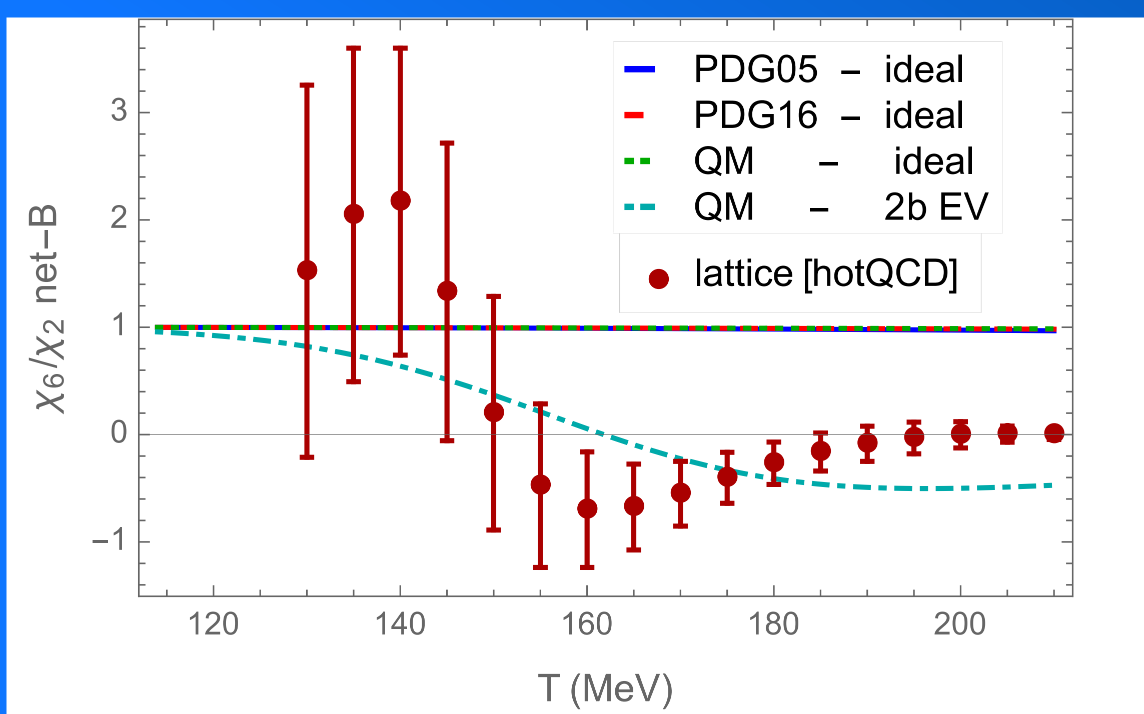

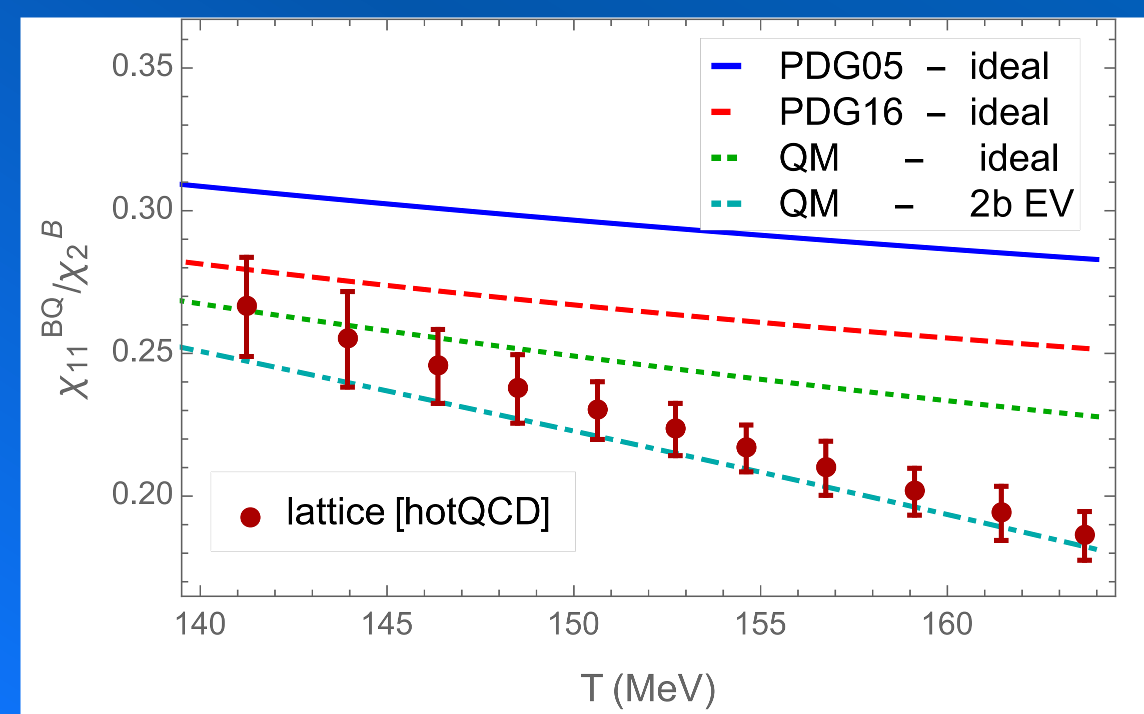

EV + QM: predictions

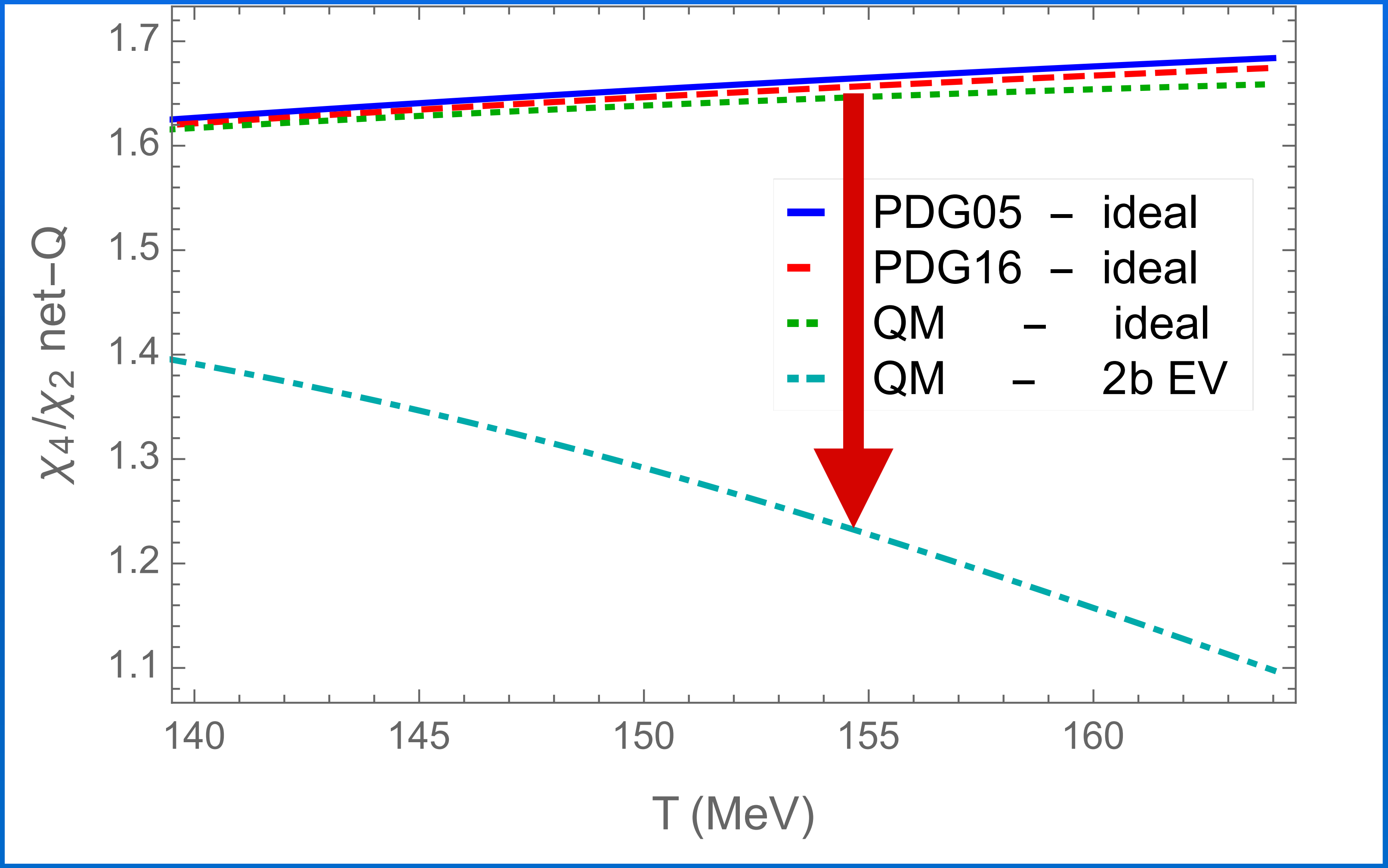

EV + QM: predictions

ALICE data: are errors small enough?

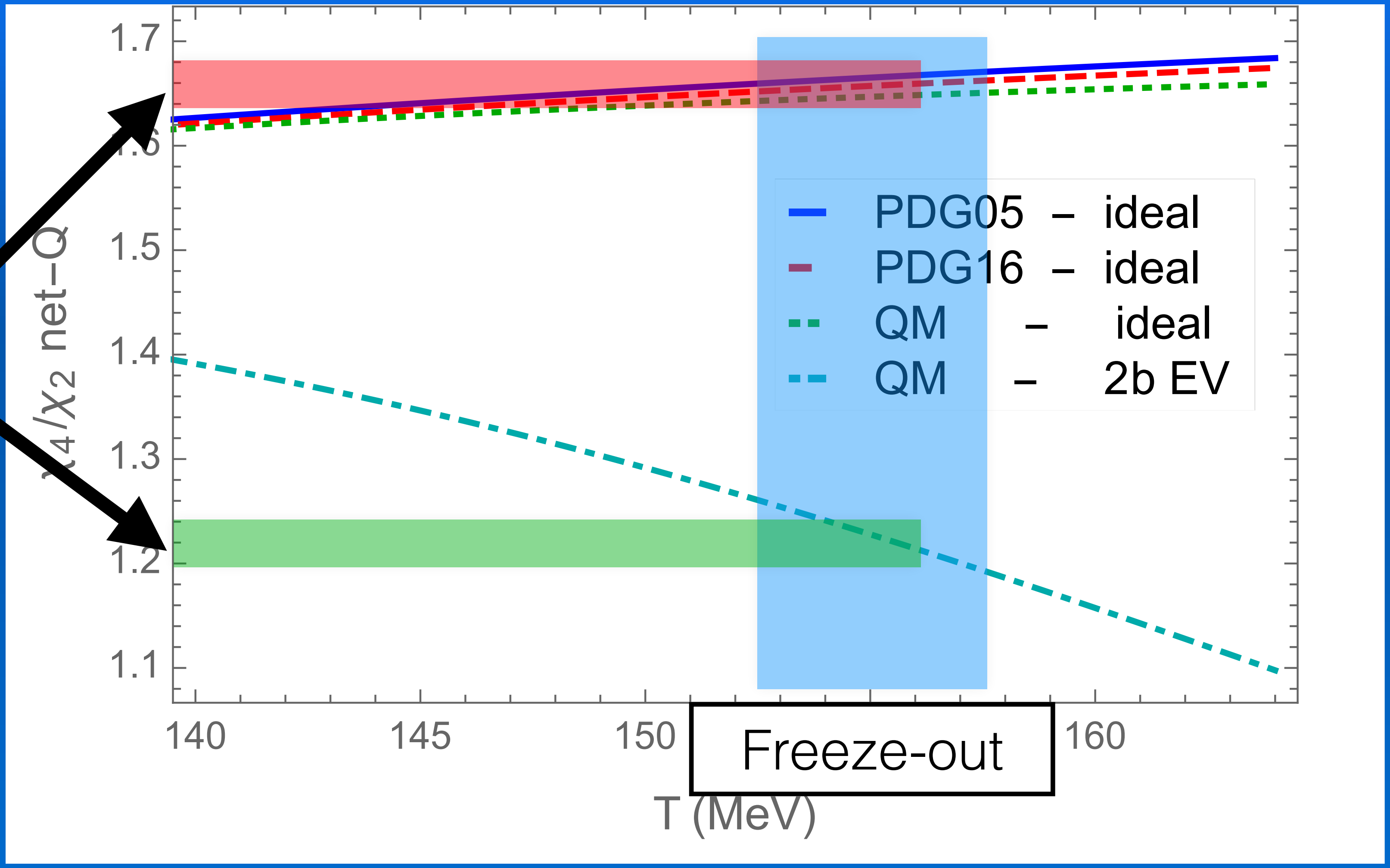

EV + QM: yields

ALICE@2.76 TeV

	PDG14	QM
id	χ^2/N_{dof}=20/9≃2.2 T= 155.2±2.2 (MeV) μ_B= 3.8±7 (MeV) V= 4663.1±590.3 (fm ^{3})	χ^2/N_{dof}=11.4/9≃1.2 T= 148.3±1.8 (MeV) μ_B= 6.9±7.2 (MeV) V= 6182.7±710.4 (fm ^{3})
2b		χ^2/N_{dof}=12.8/9≃1.42 T= 149.4±1.78 (MeV) μ_B= 7.6±7.79 (MeV) V= 7323.8±694.6 (fm ^{3})

STAR@200 GeV

	PDG14	QM
id	χ^2/N_{dof}=14.1/8≃1.8 T= 164.1±2.3 (MeV) μ_B= 29.6±8.4 (MeV) V= 1492.1±187.8 (fm ^{3})	χ^2/N_{dof}=7.4/8≃0.9 T= 157.0±1.9 (MeV) μ_B= 31.1±8.3 (MeV) V= 1934.9±232.6 (fm ^{3})
2b		χ^2/N_{dof}=11.9/8≃1.48 T= 156.4±1.75 (MeV) μ_B= 30.95±8.6 (MeV) V= 2744.1±239.5 (fm ^{3})

For both energies are used the parameters extracted from the fit to lattice QCD.

EV + QM: yields

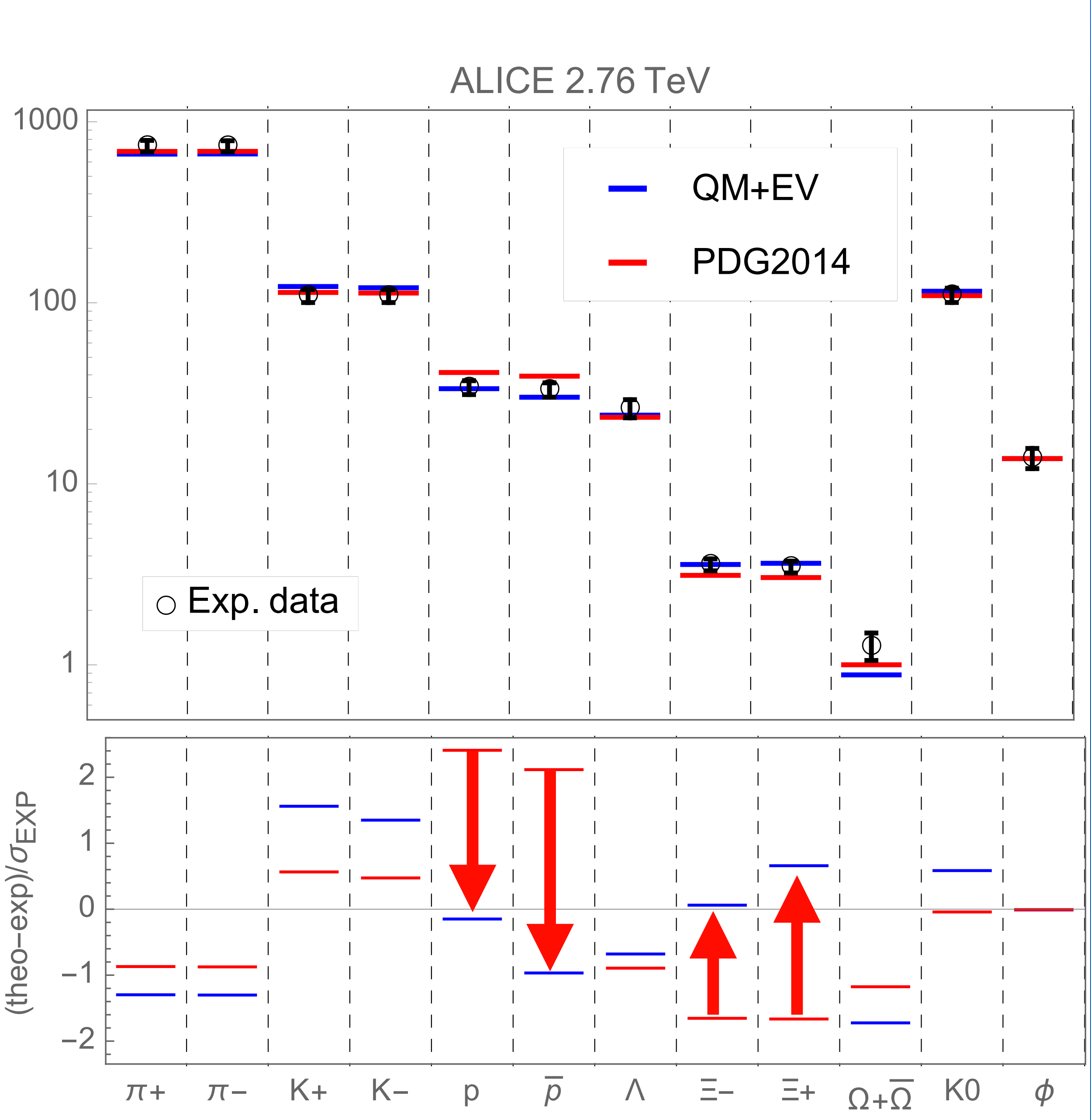
ALICE 2.76 TeV
QM+EV
PDG2014
○ Exp. data
1000
100
10
1
(theo−exp)/σEXP
2
1
0
−1
−2
π+
π−
K+
K−
p
p̄
Λ
Ξ−
Ξ+
Ω+Ω̄
K0
ϕ

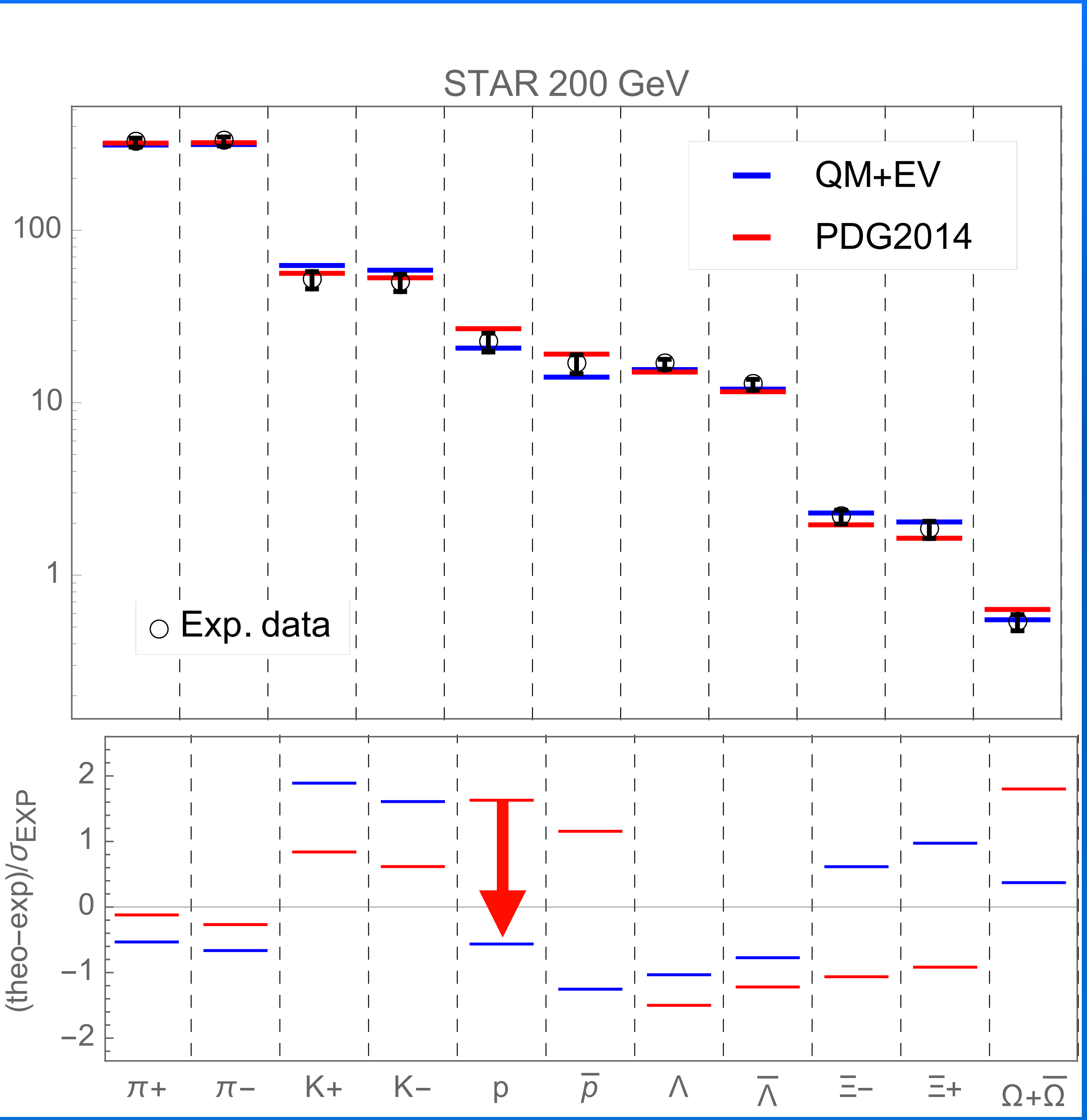
STAR 200 GeV
QM+EV
PDG2014
○ Exp. data
100
10
1
(theo−exp)/σEXP
2
1
0
−1
−2
π+
π−
K+
K−
p
p̄
Λ
Λ̄
Ξ−
Ξ+
Ω+Ω̄

Conclusions

- Higher order moments of particle multiplicity distributions can be directly compared to lattice
- There are inconsistencies in the hadronic spectrum, which can be interpreted as missing resonances
- EV effects are an useful tool in order to parametrise effective hadronic interactions
- There are signatures for smaller strange states, both from lattice thermodynamics and particle yields.

Thanks for your attention

Flavor hierarchy

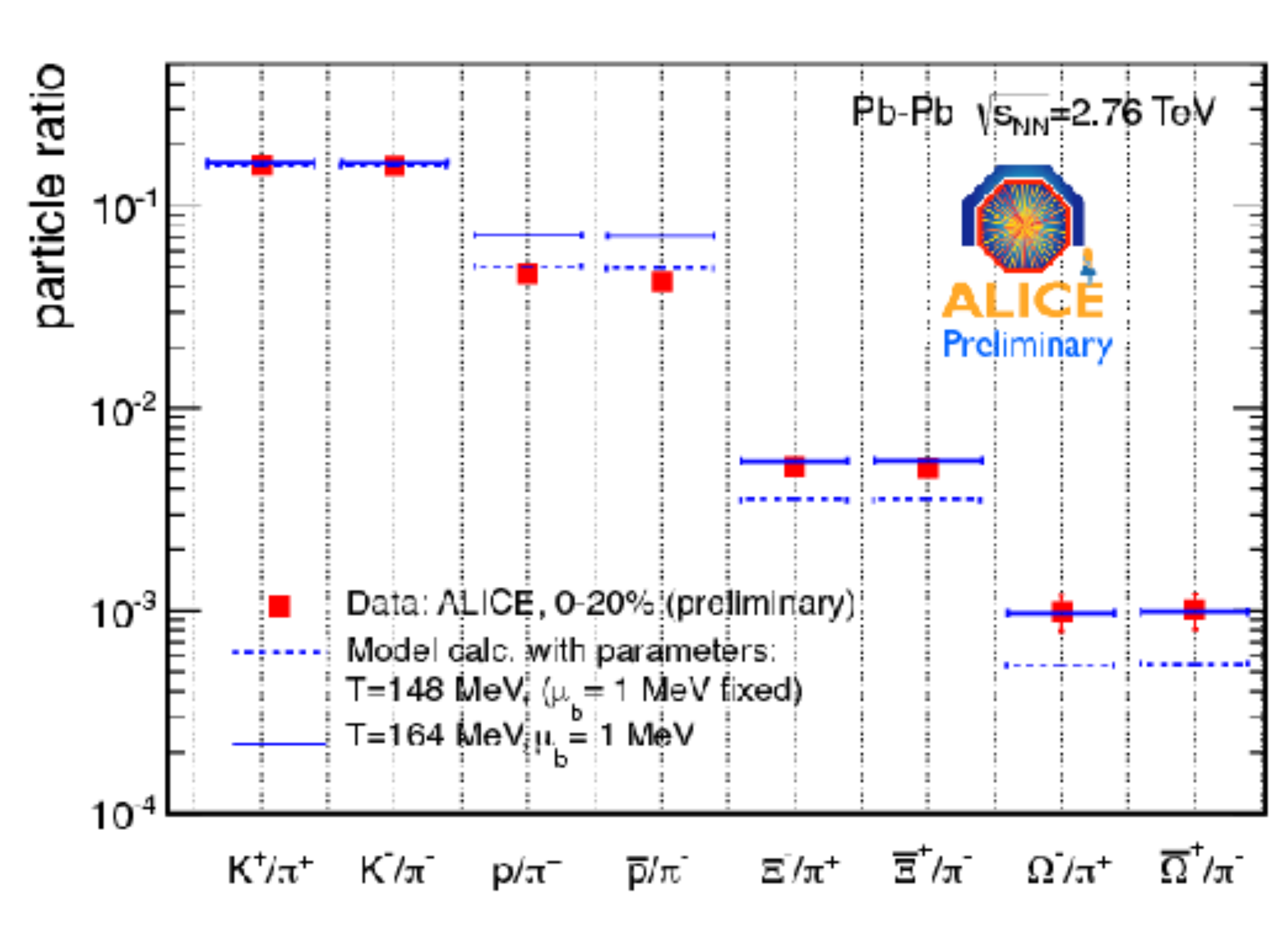

Preghenella, Acta Phys.Polon. B43 (2012) 555

EV: crosstersm

This version of the model is consistent with the 2nd order viral expansion. The number of free parameters does not change.

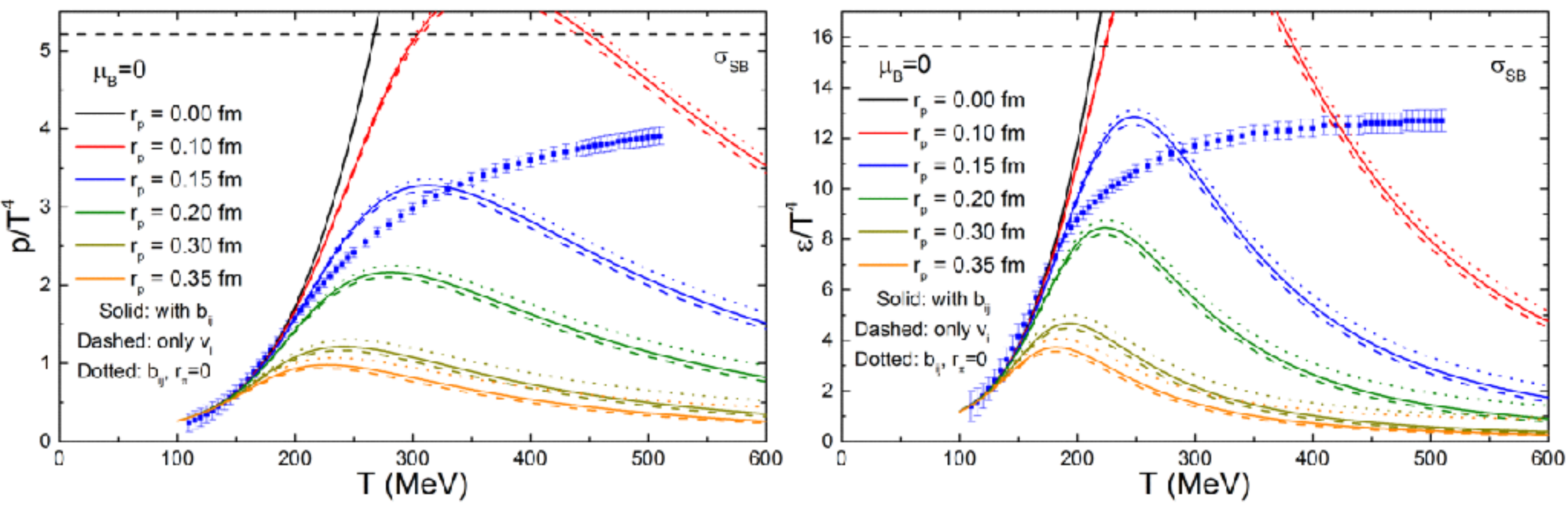

EV: crosstersm

This version of the model is consistent with the 2nd order viral expansion. The number of free parameters does not change.

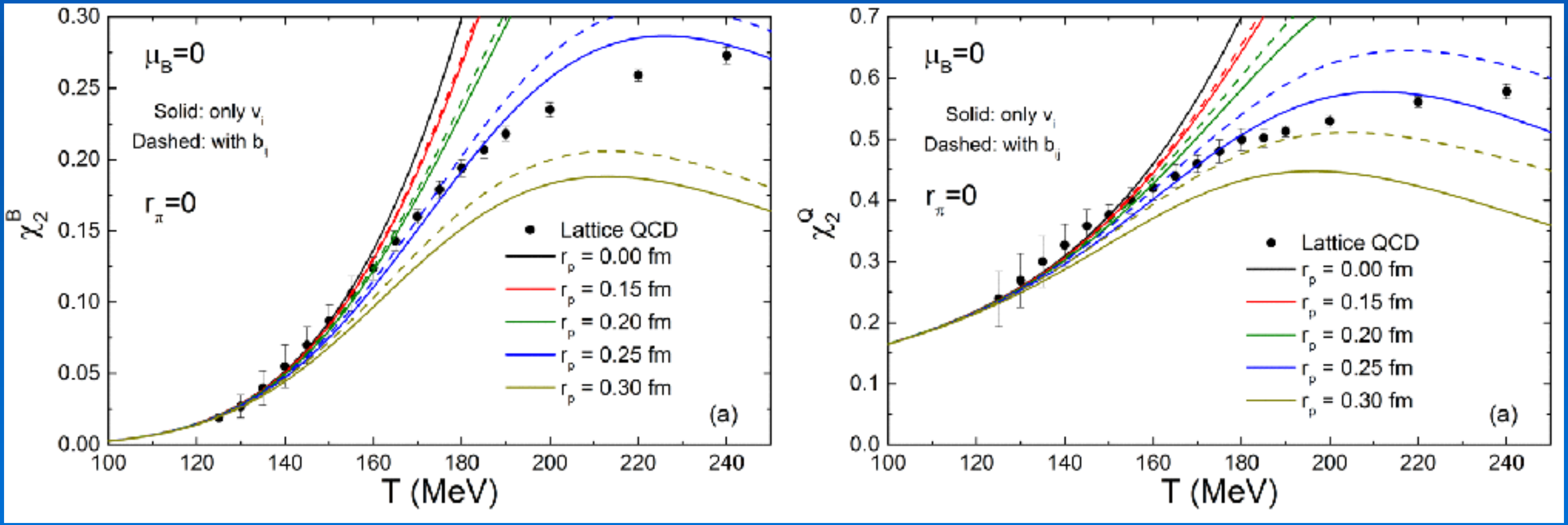

EV: particle yields

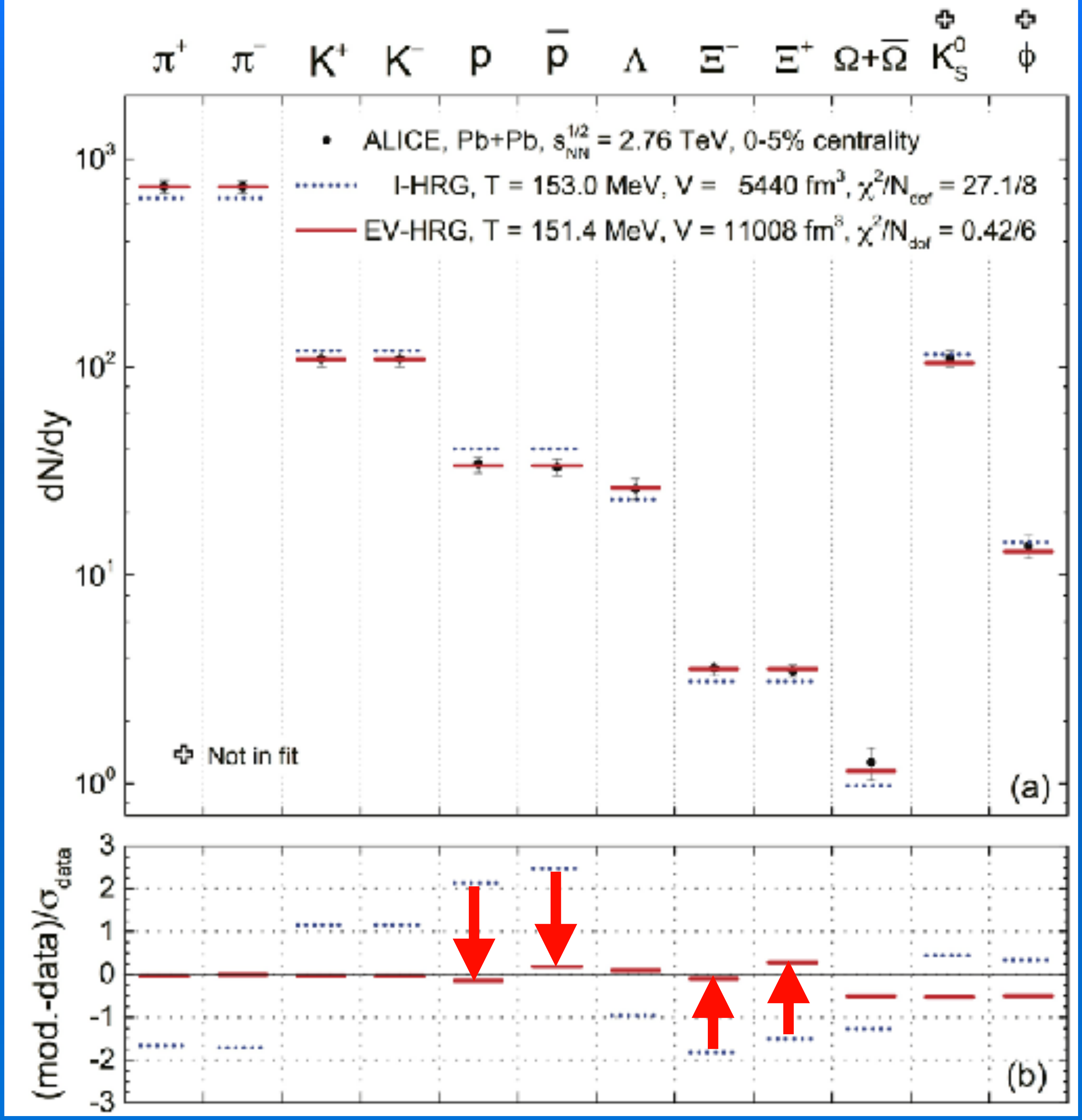

A detailed balance of particle suppression removes the so called proton anomaly.

P.A. et al. arxiv: hep-ph 1606.06542

EV: particle yields

With the parameters extracted from ALICE 0-5%, there is an overall improvement for all centralities and lower energies.

	χ^2/Ndf p.l.	χ^2/Ndf	T (MeV) p.l.	T (MeV)
ALICE 0-5%	2.642537	0.0985746	152.576606	150.270412
ALICE 5-10%	4.038844	0.082681	153.855798	151.702161
ALICE 10-20%	4.831962	0.187238	156.912643	153.761281
ALICE 20-30%	5.779079	0.505264	156.269898	155.342295
ALICE 30-40%	5.290277	0.479082	156.606086	155.778665
ALICE 40-50%	4.320371	0.225175	156.901153	155.046625
ALICE 50-60%	2.528466	0.431904	153.374355	152.640780
ALICE 60-70%	2.522801	0.896884	148.338287	150.736294
ALICE 70-80%	2.480648	0.516741	150.701703	158.829787

	χ^2/Ndf p.l.	χ^2/Ndf	T (MeV) p.l.	T (MeV)
NA49 20GeV	5.868216	3.668726	106.448226	122.919464
NA49 30GeV	7.222598	1.269705	141.555846	136.454728
NA49 40GeV	8.077212	2.292649	139.293714	136.775614
NA49 80GeV	13.783130	4.812104	138.121797	141.917805
NA49 158GeV	5.329034	1.590537	146.535995	142.932057

There are no relevant changes in the freeze-out parameters.